



## Transportation Science

Publication details, including instructions for authors and subscription information:  
<http://pubsonline.informs.org>

### Differentiated Pricing of Shared Mobility Systems Considering Network Effects

Matthias Soppert, Claudius Steinhardt, Christian Müller, Jochen Gönsch

To cite this article:

Matthias Soppert, Claudius Steinhardt, Christian Müller, Jochen Gönsch (2022) Differentiated Pricing of Shared Mobility Systems Considering Network Effects. *Transportation Science* 56(5):1279-1303. <https://doi.org/10.1287/trsc.2022.1131>

Full terms and conditions of use: <https://pubsonline.informs.org/Publications/Librarians-Portal/PubsOnLine-Terms-and-Conditions>

This article may be used only for the purposes of research, teaching, and/or private study. Commercial use or systematic downloading (by robots or other automatic processes) is prohibited without explicit Publisher approval, unless otherwise noted. For more information, contact [permissions@informs.org](mailto:permissions@informs.org).

The Publisher does not warrant or guarantee the article's accuracy, completeness, merchantability, fitness for a particular purpose, or non-infringement. Descriptions of, or references to, products or publications, or inclusion of an advertisement in this article, neither constitutes nor implies a guarantee, endorsement, or support of claims made of that product, publication, or service.

Copyright © 2022 The Author(s)

Please scroll down for article—it is on subsequent pages



With 12,500 members from nearly 90 countries, INFORMS is the largest international association of operations research (O.R.) and analytics professionals and students. INFORMS provides unique networking and learning opportunities for individual professionals, and organizations of all types and sizes, to better understand and use O.R. and analytics tools and methods to transform strategic visions and achieve better outcomes.




For more information on INFORMS, its publications, membership, or meetings visit <http://www.informs.org>

# Differentiated Pricing of Shared Mobility Systems Considering Network Effects

Matthias Soppert,<sup>a,\*</sup> Claudius Steinhardt,<sup>a</sup> Christian Müller,<sup>b</sup> Jochen Gönsch<sup>b</sup>

<sup>a</sup>Chair of Business Analytics and Management Science, University of the Bundeswehr Munich, 85577 Neubiberg, Germany; <sup>b</sup>Chair of Service Operations, University of Duisburg-Essen, 47057 Duisburg, Germany

\*Corresponding author

Contact: matthias.soppert@unibw.de,  <https://orcid.org/0000-0003-3399-0525> (MS); claudius.steinhardt@unibw.de,  <https://orcid.org/0000-0003-4263-6608> (CS); christian.mueller.9@uni-due.de,  <https://orcid.org/0000-0002-2950-446X> (CM); jochen.goensch@uni-due.de,  <https://orcid.org/0000-0002-5699-1320> (JG)

Received: September 9, 2020

Revised: May 27, 2021; November 9, 2021


Accepted: December 22, 2021

Published Online in Articles in Advance:  
April 1, 2022

<https://doi.org/10.1287/trsc.2022.1131>

Copyright: © 2022 The Author(s)

**Abstract.** Over the last decades, shared mobility systems have become an integral part of inner-city mobility. Modern systems allow one-way rentals, that is, customers can drop off the vehicle at a different location to where they began their trip. A prominent example is car sharing. Indeed, this work was motivated by the insight we gained in collaborating closely with Europe's largest car sharing provider, Share Now. In car sharing, as well as in shared mobility systems in general, pricing optimization has turned out to be a promising means of increasing profit while challenged by limited vehicle supply and asymmetric demand across time and space. Thus, in practice, providers increasingly use minute pricing that is differentiated according to where a rental originates, that is, considering its location and the time of day. In research, however, such approaches have not been considered yet. In this paper, we therefore introduce the corresponding origin-based differentiated, profit-maximizing pricing problem for shared mobility systems. The problem is to determine spatially and temporally differentiated minute prices, taking network effects on the supply side and several practice relevant aspects into account. Based on a deterministic network flow model, we formulate the problem as a mixed-integer linear program and prove that it is NP-hard. For its solution, we propose a temporal decomposition approach based on approximate dynamic programming. The approach integrates a value function approximation to incorporate future profits and account for network effects. Extensive computational experiments demonstrate the benefits of capturing such effects in pricing generally, as well as showing our value function approximation's ability to anticipate them precisely. Furthermore, in a case study based on Share Now data from Florence in Italy, we observe profit increases of around 9% compared with constant uniform minute prices, which are still the de facto industry standard.

 **Open Access Statement:** This work is licensed under a Creative Commons Attribution 4.0 International License. You are free to copy, distribute, transmit and adapt this work, but you must attribute this work as "Transportation Science. Copyright © 2022 The Author(s). <https://doi.org/10.1287/trsc.2022.1131>, used under a Creative Commons Attribution License: <https://creativecommons.org/licenses/by/4.0/>."

**Funding:** This work was supported by the University of the Bundeswehr Munich.

**Supplemental Material:** The online appendices are available at <https://doi.org/10.1287/trsc.2022.1131>.

**Keywords:** shared mobility systems • car sharing • differentiated pricing • origin-based pricing • supply-side spatio-temporal network effects • approximate dynamic programming • optimization

## 1. Introduction

Shared mobility systems (SMSs) such as car sharing or bike sharing offer flexible short-term rentals in many major cities of the world. Globally, the number of car sharing vehicles has increased from 11,500 in 2006 to 112,000 in 2015, with 427,000 cars forecast for 2025 (ACEA Frost & Sullivan 2016). In terms of annual growth, projections for the global car sharing market were recently at 30%. Also, bike sharing systems have experienced a strong market growth of 20% per year (Roland Berger 2014). Their increasing importance, as well as the

challenge to operate such systems profitably, have led to an ongoing academic interest, as survey papers by Jorge and Correia (2013) and Laporte, Meunier, and Wolfler Calvo (2018), among others, demonstrate.

Because the fleet is the most important cost driver, high utilization is key to profitably operating an SMS. This, however, is difficult to achieve because of existing *imbalances* between supply and demand. First, customers' demand varies across time and space. Second, a rental not only instantly decreases available capacity at its origin but also influences future supply

across the whole system. These *supply-side network effects* result from the fact that modern systems mostly allow one-way trips; that is, the customer does not need to return the vehicle to the same location as where the trip originated. A practical consequence is that in most real-world systems, because of asymmetric demand, rental vehicles tend to accumulate at certain locations, usually in the city's outskirts.

The described imbalances are widely addressed by supply-oriented operational control mechanisms such as vehicle relocation. However, as relocations are quite costly, pricing has been identified as a promising demand-oriented means in practice and in research. Most recently, Huang et al. (2020) compare relocation and pricing optimization (also see Di Febbraro, Sacco, and Saeednia 2012; Jorge, Molnar, and Correia 2015; Lippoldt, Niels, and Bogenberger 2018, 2019). Although the existing research tends to focus on pricing problems with a high degree of details and high pricing flexibility, current practical implementations strive for simple, more restrictive pricing mechanisms that are more easily applied and communicated to customers. Interestingly, the restriction to simple pricing mechanisms while network effects prevail turns out to create its own challenges.

Three dimensions characterize pricing mechanisms for SMSs, all of which impact the mentioned tradeoff between flexibility and practicability, as explicated here.

- *Pricing basis*: The first pricing dimension concerns the basis on which rental fees are calculated. The rental duration is usually central. *Usage-based pricing*, for example with prices in cents per minute, is most commonly used and therefore we focus on this in our work. The final rental fee is then determined by the rental duration and the price that is valid at the start of the journey. In addition, some SMS providers offer *package pricing* for long rentals of multiple hours, fixed rental fees, or monthly membership fees that are not linked to usage.

- *Spatio-temporal pricing features*: The second pricing dimension refers to whether the SMS provider sets prices depending on a rental's time and the location of start (origin), end (destination), or a combination of these (trip). In this terminology, origin and destination consider both spatial and temporal aspects, that is, two rentals that begin at the same location but at different times of the day have different origins. *Trip-based pricing* mechanisms use prices that depend on origin and destination, allowing a very detailed level of pricing. By contrast, *origin-based* and *destination-based* mechanisms only depend on the origin or destination, respectively. Although trip-based pricing may seem most powerful, there are several practical disadvantages. First, the customer's destination is usually unknown in advance (Lippoldt, Niels, and Bogenberger 2018,

2019). Second, pricing mechanisms that include the destination become much more complicated (Lippoldt, Niels, and Bogenberger 2018). Third, prices need to be transparently communicated to the customer before a rental. Attempts to prepare all origin-destination combinations in a price table are impractical. The SMS provider then would have to ask a user to (truthfully) disclose the intended destination, which would considerably change the user experience of most real SMSs and thus would be unacceptable in most practical settings. Because of these drawbacks, trip-based pricing seems not to be realizable in practice, and we are not aware of a single SMS provider who has actually implemented such trip-based pricing (see Online Appendix I). This paper therefore focuses on origin-based pricing as a mechanism most commonly used in current practice, because the SMS provider then requires less information than otherwise. It also entails a more efficient user-provider interaction process and fairly simple implementation.

- *State dependency*: The third pricing dimension distinguishes between dynamic and differentiated pricing. *Dynamic pricing* mechanisms determine prices in real-time and have the theoretical advantage of recurrently adjusting prices to the current state of the system, in particular, the current spatial vehicle distribution. *Differentiated pricing* mechanisms also allow for temporal and spatial price variations, but prices are determined offline and do not depend on the current state of the system (Agatz et al. 2013). Some authors use the term static pricing for this pricing mechanism (Waserhole and Jost 2012). For SMSs, these differentiated pricing mechanisms, on which we focus in this paper, are preferred in practice. This is mainly because differentiated mechanisms are easier to implement and again, quite importantly, easy to communicate transparently to customers, for example, via price tables.

The problem we consider in this paper can therefore be summarized as follows: A one-way SMS provider applies *origin-based differentiated pricing* by varying minute prices across different locations and depending on the time of day to scale demand. Consistent with the common situation in practice, there are no parallel operational steering means beyond pricing (*pure pricing assumption*). In particular, there is no availability control; that is, whenever vehicle and customer match, a rental results. However, if at a certain location and point in time, demand exceeds supply, demand for all destinations is served proportionally (*proportional demand fulfillment assumption*) and excess demand is lost. This can be interpreted as customers with different destinations arriving in random order. Resulting rentals evoke network effects in the aforementioned sense of influencing supply at their destinations later in the day. To ensure simple and transparent customer communication, prices must originate from a predefined discrete price set.

Given this setting, the optimization task is now to set prices optimally for all location-time combinations, with the SMS provider's overall objective being profit maximization. We refer to this optimization problem as the *origin-based differentiated pricing problem* (OBDPP) in SMSs.

Given its broad relevance to practice and across all SMS types, it is remarkable that the problem has not yet been addressed in the academic literature. Our contributions, more precisely, are the following:

- To the best of our knowledge, we are the first to focus on origin-based differentiated pricing, which is highly relevant for various SMS types in practice because the corresponding pricing mechanism is transparent to the customer and relatively easy for the provider to implement. In addition, we include other novel problem characteristics such as a realistic modeling of the SMS provider's control ability. The problem's practical relevance is ensured by, among other things, close cooperation we have established with Share Now, Europe's largest car sharing provider operating in eight countries and 16 cities (Share Now 2021).

- Second, we prove that the problem is NP-hard and therefore computationally intractable for real-life instances. Although some authors (Waserhole and Jost 2012, Ren et al. 2019) discuss the computational effort SMS pricing problems require, to the best of our knowledge, we are the first to derive a formal proof of computational complexity for such a problem to validly justify the development of solution heuristics.

- Third, we develop a problem-specific, temporal decomposition heuristic based on approximate dynamic programming (ADP). The approach is scalable and applicable to real-world problems. Its integrated value function approximation (VFA) anticipates the network effects of the entire problem endogenously in the optimization, although only parts of the original problem are explicitly optimized during the decomposition. This is enabled by specifying piece-wise linear VFAs that reflect the available vehicles' decreasing marginal value while maintaining linearity for efficiently integrating it in the decomposed optimization problems.

- Fourth, we generate a number of relevant managerial insights based on extensive computational experiments with different problem sizes, considering many relevant parameter settings and demand patterns, and on a real-world case study of Share Now. In particular, we demonstrate that origin-based pricing is capable of substantially increasing profit compared with the de facto industry standard of constant uniform pricing. Furthermore, we show that our approach can adequately capture both short-term and long-term network effects because of its VFA.

The remainder of the paper is organized as follows. In Section 2, we review the relevant literature, focusing on pricing problems. In Section 3, we formalize

the origin-based differentiated pricing problem, derive its model formulation, and discuss its complexity. We present the proposed solution approach in Section 4. Section 5 contains the computational experiments, and Section 6 presents the Share Now case study. Based on the obtained results, Section 7 discusses the managerial insights we derived. Section 8 concludes the paper and gives an outlook on future research. The appendix contains the complexity proof, as well as additional data and results for the computational experiments and case study.

## 2. Literature Review

General overviews on SMS problems have been given in survey papers on bike sharing (DeMaio 2009, Fishman, Washington, and Haworth 2013, Ricci 2015), car sharing (Jorge and Correia 2013; Ferrero et al. 2015a, b; Illgen and Höck 2019), and shared mobility in general (Laporte, Meunier, and Wolfler Calvo 2015, 2018). We begin by reviewing the literature on differentiated pricing problems in Section 2.1 and dynamic pricing problems in Section 2.2. Then, we give a detailed delineation of our work from the papers most closely related in Section 2.3. Please note that because most pricing mechanisms are not limited to a single SMS type like bike sharing or car sharing, we refrain from mentioning whether the authors considered a specific SMS type. Also, we do not state explicitly whether the authors considered other optimization problems besides pricing, such as fleet sizing or relocation.

### 2.1. Differentiated Pricing

The literature on optimizing differentiated pricing for SMSs focuses on trip-based pricing.

Waserhole and Jost (2012) propose a fluid approximation for the revenue-maximizing trip-based pricing problem, which is the limit of the stochastic model when demand and supply are scaled to infinity. In another paper from the same research group, Waserhole, Jost, and Brauner (2012) present a model optimizing revenue in a single scenario; that is, they focus on solving the discrete problem with perfect hindsight information. This can be used to derive an upper bound for the stochastic problem. They also consider pick-up and drop-off fees. To our knowledge, this paper is the only one in the related literature that has investigated computational complexity.

The following papers apply a certainty equivalent approach that replaces stochastic quantities (i.e., rentals) with a deterministic value (Bertsekas 2019, chapter 2.3.2). Jorge, Molnar, and Correia (2015) use a continuous (expected) demand function and round rentals to the next integer value in the model. They formulate a profit-maximizing trip-based pricing problem as mixed-integer nonlinear program and propose an iterated local

search meta-heuristic solution approach. Building on this work, Ren et al. (2019) integrate the vehicle-grid interaction of electric vehicles into the model and use a nonlinear solver for the resulting problem. The next two papers simply require rentals to be integral values not exceeding a continuous demand function. Xu, Meng, and Liu (2018) formulate a mixed-integer nonlinear and nonconvex program. On this basis, they develop a computationally tractable convex model that has the same objective in the optimum and solve the latter arbitrarily close to optimality. Huang et al. (2020) use a deterministic, continuous demand function. They discuss two pricing approaches that they compare with relocation. Although the first is a classic trip-based pricing approach, the second involves simultaneously optimizing pick-up and drop-off fees. They formulate mixed-integer nonlinear programs and solve them with a combined rolling horizon and iterated local search heuristic, which the authors point out can also be applied in a dynamic context.

Lu et al. (2021) use yet another formulation, that is, a bilevel nonlinear program based on a fluid approximation in which the provider determines profit-maximizing prices on the upper level. The lower level's objective minimizes customers' total cost by a binary choice between two modes of transportation, namely shared vehicles and private cars. In an unusual interpretation of a discrete choice model, rentals are additionally bounded from above by a logit model. The authors transform the bilevel problem to a single-level one using Karush-Kuhn-Tucker conditions and heuristically solve it with a genetic algorithm.

Finally, there are two other more distant lines of work, parallel to the aforementioned. One analytically investigated the steady state of highly stylized, stationary settings with time-invariant demand using techniques from closed-queuing networks. Waserhole and Jost (2016) maximize the number of trips taken, assuming null travel time. They approximate the problem and show a bound for the solution quality. Banerjee, Freund, and Lykouris (2021) basically extended this result using a different proof and approximation techniques. A second parallel line of work considered pricing in SMSs but without optimization. For example, Brendel et al. (2017) developed a framework for a decision support system that could help to define contingent areas with low or high demand. The provider can then manually choose pick-up and drop-off discounts and fees for these areas.

## 2.2. Dynamic Pricing

Dynamic pricing problems make up most pricing problems considered in the literature on SMSs. We structure the discussion along the spatio-temporal pricing features (second dimension introduced in

Section 1). We begin with the dynamic mechanisms that exclusively use either origin-based or destination-based pricing. Next, we refer to a class of approaches that simultaneously considers dynamic origin- and destination-based pricing, after which we discuss those using classic trip-based pricing.

Giorgione, Ciari, and Viti (2019) are the first scholars to have considered pure origin-based dynamic pricing. They analyze a dynamic pricing policy that links the price to the availability of vehicles at a rental's origin and demonstrate the advantage of dynamic pricing over a constant uniform price. Neijmeijer et al. (2020) propose an optimization model that dynamically adjusts prices with the objective to balance vehicles' idle times while minimizing incentive costs. In a real-life free-floating SMS, the authors demonstrate the effectiveness of origin-based pricing incentives. Most recently, Hardt and Bogenberger (2021) and Müller et al. (2021) proposed dynamic origin-based pricing approaches for free-floating SMSs, both with the objective to maximize profit. The former uses a model predictive control approach that recurrently optimizes prices for subareas of the operating area. The latter proposes customer-centric pricing where prices are optimized individually for each customer, thereby considering the available vehicles within a customer's reach and the choice behavior.

Destination-based dynamic pricing was first investigated by Di Febbraro, Sacco, and Saeednia (2012). In a first step, they determine a service maximizing fleet distribution, whereas the second step determines optimal drop-off discounts that incentivize customers to return their vehicle to a specific destination. Following up on this work, Di Febbraro, Sacco, and Saeednia (2019) changed the second step's objective to profit maximization. Brendel, Brauer, and Hildebrandt (2016) proposed a dynamic drop-off incentive for users who accept the option of returning their vehicle to a different location than that initially intended. Pfrommer et al. (2014) suggest a model predictive control approach. The objective is a weighted sum of the deviation from an optimal vehicle distribution and the cost of incentive payments. Wagner et al. (2015) propose a system that dynamically suggests alternative rental destinations and incentivizes customers with free minutes. Chemla et al. (2013) consider a service maximizing fleet utilization, measured by successful and unsuccessful intended customer interactions like finding an available vehicle. They suggest dynamic drop-off fees to influence customer behavior. Marecek, Shorten, and Yu (2016) propose a dynamic pricing scheme that derives drop-off fees to incentivize drivers to distribute cars more evenly.

Some authors simultaneously consider dynamic origin- and destination-based pricing. Singla et al. (2015) investigate the problem of minimizing customers' dissatisfaction

about not finding an available vehicle or parking slot under a given budget restriction. They propose dynamic pick-up and drop-off fees to incentivize users to choose an alternative origin or destination. Kamatani, Nakata, and Arai (2019) take a reinforcement learning approach to derive dynamic pick-up and drop-off fees with the objective of maximizing fleet utilization. Wang and Ma (2019) consider the objective of keeping inventories in a certain range, and they determine dynamic pick-up and drop-off rewards and charges by a quadratic programming formulation.

Finally, there are papers that use a dynamic trip-based pricing mechanism. Barth, Todd, and Xue (2004) consider maximizing fleet utilization by incentivizing customers with the same journey to share a ride or to split up and use multiple vehicles. Prices are reduced according to a simple rule-based mechanism without any optimization. For example, if two users are asked to take two cars, each pays half-price. Angelopoulos et al. (2016) consider the problem of dynamically setting budget-constrained trip-based incentives in an SMS to balance the vehicle inventory. The approach uses graph-theoretic modeling and proposes a heuristic method to solve the resulting weighted packing problem. Haider et al. (2018) dynamically set trip-based prices to minimize the number of unbalanced stations, that is, SMS stations with a surplus or lack of vehicles, to ease the subsequent need to reposition using trucks. In their bilevel programming approach, the upper level sets prices and minimizes the imbalance, whereas the lower level represents customers' cost minimization route choices. They convert the problem to a single-level problem and propose a heuristic that iteratively adjusts prices and customer decisions.

### 2.3. Delineation from Closest Related Work

In this section, we discuss that the closest related works cannot be simply adapted to meet the given characteristics of the origin-based differentiated pricing problem this paper considers.

Among the papers discussed here, which all focus on trip-based pricing, we identify two groups that differ regarding the modeling of demand and rentals. For both groups, we conclude that central structural differences impede an inclusion of the OBDPP's characteristics.

The first group of papers does not distinguish between demand and rentals. It encompasses Jorge, Molnar, and Correia (2015), Ren et al. (2019), Waserhole and Jost (2012), and Haider et al. (2018), who study differentiated and dynamic trip-based pricing. The former three consider unrestricted, continuous prices that scale demand. Thus, it is always optimal to set prices such that capacity is not scarce and therefore that demand will equal rentals. The key issue is that,

with the restricted and especially discrete price points prevalent in practice, this equivalence of demand and rentals no longer holds and is usually even infeasible. Allowing for discrete prices requires a differentiation between demand and rentals, as well as explicitly incorporating the *pure pricing* and *proportional demand fulfillment assumptions*. Thus, it would require major modeling changes.

By contrast, Haider et al. (2018) do not scale demand by continuous prices; they only influence customers' route choices in a bilevel problem with an infinite fleet size. Moreover, their model is optimistic, that is, if customers are indifferent, the provider chooses the itinerary for them. Although including discrete prices with demand scaling, profit maximization, and origin-based pricing in their model seems possible, this alone would yield an entirely new model. However, there are two key issues. First, incorporating a limited fleet size would also necessitate accounting for the *pure pricing assumption*. Second, the problem that we consider with its *proportional demand fulfillment assumption* is neither optimistic nor pessimistic. As optimistic approaches are usually the most tractable ones, including these two assumptions appears to be complex.

The second group of papers encompasses Xu, Meng, and Liu (2018), Lu et al. (2021), and Huang et al. (2020), who distinguish between demand and rentals in their models, but do not satisfy the *pure pricing* and *proportional demand fulfillment assumptions*. Xu, Meng, and Liu (2018) and Huang et al. (2020) include demand scaling with continuous prices. Their models bound rentals only from above by supply and demand. Thus, the provider can freely choose the number of rentals going to the different destinations up to these bounds, as it is beneficial in the long term. This violates the *pure pricing* and *proportional demand fulfillment assumptions*. An extension of their models that includes the assumptions in respective constraints seems possible, but the changes would be so extensive that basically any network flow model could be used.

Slightly similar to Haider et al. (2018), Lu et al. (2021) do not scale total demand by continuous prices, but only influence customers' mode choices on the lower level of their bilevel problem, where they work with the assumption of customers collectively minimizing cost. As in Haider et al. (2018), the key issue is that the model is optimistic. If customers' costs are the same for carsharing and private cars on a trip, the provider can choose the number of customers up to the logit model's bound. Even more importantly, if this holds for several trips, the provider can freely choose the number of customers for each trip. Again, there is no clear path to include the two assumptions.

The work of Giorgione, Ciari, and Viti (2019) is not closely related. Although they do analyze a pure origin-based pricing problem, they do so without pricing optimization, without considering network effects, and in a dynamic context which fundamentally differs from the differentiated pricing problem that we analyze.

### 3. Origin-Based Differentiated Pricing Problem in Shared Mobility Systems

In this section, we define and analyze the origin-based differentiated pricing problem in SMSs (OBDPP). Section 3.1 formally states the problem and introduces the notation. In Section 3.2, we present a mixed-integer linear programming formulation for the OBDPP based on a fluid network flow model. Section 3.3 investigates the computational complexity of the problem.

#### 3.1. Problem Statement and Notation

We take the perspective of a one-way SMS provider whose task is to apply differentiated pricing to determine minute prices over a given time interval, for example, one day. The SMS consists of locations  $\mathcal{Z} = \{1, 2, \dots, Z\}$ . The considered time interval is discretized into periods  $\mathcal{T} = \{0, 1, \dots, T-1\}$ . For all rentals that originate at a specific combination of location  $i \in \mathcal{Z}$  and period  $t \in \mathcal{T}$ , the same minute price  $p_{it}$  is charged, regardless of a trip's destination (origin-based pricing). The minute prices have to be selected from  $M$  given price points  $p^m \in \mathbb{R}_0^+$  with  $m \in \mathcal{M} = \{1, 2, \dots, M\}$ . Now, the provider's objective is to set the prices such that they maximize the profit generated from the resulting rentals over the given time interval. The corresponding solution to the problem, that is, the optimized prices, can be presented in the form of a price table, as shown in Table 1.

On a more detailed level, additional key aspects of the problem definition are the assumptions regarding demand, rental realization, and system dynamics, which we now discuss in more detail.

- *Demand:* We considered the demand and its dependence on the price points on an aggregate level as described, for example, in Talluri and van Ryzin (2004, chapter 7.3). More specifically, the base demand for every location-location-time combination, from

location  $i$  to location  $j$  at period  $t$ , is given by  $d_{ijt} \in \mathbb{R}_0^+$  and builds the base demand matrix  $\mathbf{d} = [d_{ijt}]_{\mathcal{Z} \times \mathcal{Z} \times \mathcal{T}}$ . Each entry is scaled by an  $i$ - $j$ - $t$  specific sensitivity factor  $f_{ijt}^m$ , depending on the price  $p^m$ , to obtain the actual demand  $d_{ijt}^m = d_{ijt} \cdot f_{ijt}^m$ . The price where  $f_{ijt}^m = 1$  and thereby  $d_{ijt}^m = d_{ijt}$  is denoted as base price.

- *Rental realization:* The rentals  $r_{it}^m$  that realize for a specific origin, meaning a location-time ( $i$ - $t$ ) combination, and price  $p_{it}$ , are determined by the minimum of the available vehicle count  $a_{it}$  and the prevailing actual demand, meaning  $r_{it}^m = \min(a_{it}, \sum_{j \in \mathcal{Z}} d_{ijt}^m)$ . This implicit realization of rentals based on the prevailing supply and demand implies that the SMS provider can only influence rentals via prices (*pure pricing assumption*). We assume that rentals at period  $t$  in location  $i$ , that is,  $r_{it}^m$ , split up proportionally to demand regarding their destination into the  $i$ - $j$ - $t$  specific rentals  $r_{ijt}^m$ . This means that we model  $r_{ijt}^m$  as a fraction of  $r_{it}^m$  proportional to  $d_{ijt}^m / \sum_{j \in \mathcal{Z}} d_{ijt}^m$  (*proportional demand fulfillment assumption*). We assume rentals have a variable cost per minute  $c \in \mathbb{R}_0^+$ .

- *Dynamics:* We think of the SMS dynamics as a sequential process with successive periods, as it is done in practice and commonly found in the literature, for example, in Xu, Meng, and Liu (2018). More precisely, we assume that rentals start at the beginning of a period and the vehicles, at latest, always become available again at the beginning of the respective next period. The average rental duration  $l_{ij} \in \mathbb{R}_0^+$  (in minutes) is shorter than the period length but can vary according to the spatial distance between different locations  $i$ - $j$ .

Finally, the initial vehicle distribution at the beginning of the considered time interval (beginning of the day)  $\hat{a}_{i0}$  for every location  $i$  is given as a consequence of regular relocation activity (usually performed during the night). Thus, fixed costs related to these regular relocations are out of the problem's scope.

#### 3.2. Mathematical Model

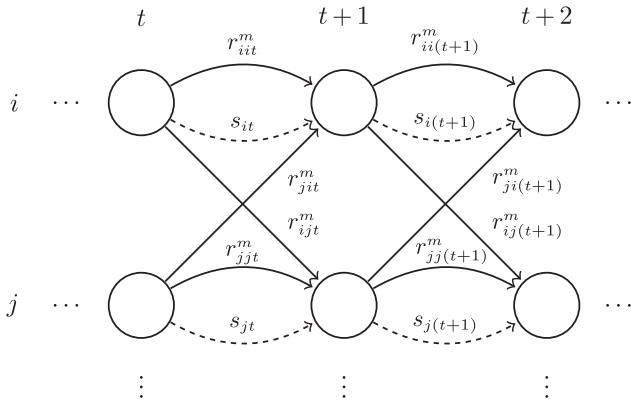
We formulate the OBDPP based on a deterministic network flow problem in which vehicles move through a spatio-temporal network (Figure 1). The resulting fluid model considers expected values of the vehicle movements and available vehicles in the SMS. Deterministic models for pricing decisions are standard in pricing and revenue management (Talluri and van Ryzin 2004, chapter 3.3.1) and are applied in SMS optimization (Waserhole and Jost 2012, Illgen and Höck 2019).

The model contains multiple continuous variables: As depicted in Figure 1, rentals from location  $i$  to location  $j$  in period  $t$  that are charged with minute price  $p^m$  are represented by the continuous variable  $r_{ijt}^m$ ; these build the elements of the vector  $\mathbf{r} = [r_{ijt}^m]_{\mathcal{Z} \times \mathcal{Z} \times \mathcal{T} \times \mathcal{M}}$ . Vehicles that are not rented in location  $i$  at period  $t$  and therefore remain in that location are represented

**Table 1.** Structure of the Origin-Based, Differentiated Price Table

$\mathcal{Z}$	$\mathcal{T}$				
	0	1	2	...	$T-1$
1	$p_{10}$	$p_{11}$	$p_{12}$	...	$p_{1(T-1)}$
2	$p_{20}$	$p_{21}$	$p_{22}$	...	$p_{2(T-1)}$
...	...	...	...	...	...
$Z$	$p_{Z0}$	$p_{Z1}$	$p_{Z2}$	...	$p_{Z(T-1)}$

**Figure 1.** Structure of the Spatio-Temporal Network



Note. Columns, time periods; rows, locations.

by the continuous variable  $s_{it}$  and are the elements of  $\mathbf{s} = [s_{it}]_{\mathcal{Z} \times \mathcal{T}}$ . The number of vehicles at the beginning of a period  $t$  in a certain location  $i$  is represented by the continuous variable  $a_{it}$  with the corresponding vector  $\mathbf{a} = [a_{it}]_{\mathcal{Z} \times (\mathcal{T}+1)}$ .

Additionally, the model contains the following binary decision variables. The pricing decisions build the elements of  $\mathbf{y} = [y_{it}^m]_{\mathcal{Z} \times \mathcal{T} \times \mathcal{M}}$ . A specific decision variable  $y_{it}^m$  takes the value of one if and only if price  $p^m$  is set in location  $i$  at period  $t$ . To formulate all necessary constraints, in particular that vehicle movements and availabilities are the result of existing demand and selected prices (see *pure pricing* and *proportional demand fulfillment assumptions* in Sections 1 and 3.1), additional auxiliary binary variables are required, represented by  $\mathbf{q} = [q_{it}]_{\mathcal{Z} \times \mathcal{T}}$ .

Based on the decision variables and the parameters defined thus far, the model can be stated as a mixed-integer linear program (MILP) as follows:

$$\max_{\mathbf{y}, \mathbf{q}, \mathbf{r}, \mathbf{a}, \mathbf{s}} \sum_{t \in \mathcal{T}} \sum_{i \in \mathcal{Z}} \sum_{j \in \mathcal{Z}} \sum_{m \in \mathcal{M}} r_{ijt}^m \cdot l_{ij} \cdot (p^m - c) \quad (1)$$

$$\text{s.t.} \quad a_{it} = \sum_{j \in \mathcal{Z}} \sum_{m \in \mathcal{M}} r_{ijt}^m + s_{it} \quad \forall i \in \mathcal{Z}, t \in \mathcal{T}, \quad (2)$$

$$\sum_{i \in \mathcal{Z}} \sum_{m \in \mathcal{M}} r_{ijt}^m + s_{jt} = a_{j(t+1)} \quad \forall j \in \mathcal{Z}, t \in \mathcal{T}, \quad (3)$$

$$a_{i0} = \hat{a}_{i0} \quad \forall i \in \mathcal{Z}, \quad (4)$$

$$\sum_{m \in \mathcal{M}} y_{it}^m = 1 \quad \forall i \in \mathcal{Z}, t \in \mathcal{T}, \quad (5)$$

$$r_{ijt}^m \leq d_{ijt}^m \cdot y_{it}^m \quad \forall i, j \in \mathcal{Z}, t \in \mathcal{T}, \quad m \in \mathcal{M}, \quad (6)$$

$$r_{ijt}^m \leq d_{ijt}^m / \sum_{k \in \mathcal{Z}} d_{ikt}^m \cdot a_{it} \quad \forall i, j \in \mathcal{Z}, t \in \mathcal{T}, \quad m \in \mathcal{M}, \quad (7)$$

$$\sum_{j \in \mathcal{Z}} \sum_{m \in \mathcal{M}} d_{ijt}^m \cdot y_{it}^m - a_{it} \leq \bar{M} \cdot q_{it} \quad \forall i \in \mathcal{Z}, t \in \mathcal{T}, \quad (8)$$

$$\sum_{j \in \mathcal{Z}} \sum_{m \in \mathcal{M}} -d_{ijt}^m \cdot y_{it}^m + a_{it} \leq \bar{M} \cdot (1 - q_{it}) \quad \forall i \in \mathcal{Z}, t \in \mathcal{T}, \quad (9)$$

$$\sum_{m \in \mathcal{M}} d_{ijt}^m \cdot y_{it}^m \leq \sum_{m \in \mathcal{M}} r_{ijt}^m + \bar{M} \cdot q_{it} \quad \forall i, j \in \mathcal{Z}, t \in \mathcal{T}, \quad (10)$$

$$s_{it} \leq \bar{M} \cdot (1 - q_{it}) \quad \forall i \in \mathcal{Z}, t \in \mathcal{T}, \quad (11)$$

$$y_{it}^m \in \{0, 1\} \quad \forall i \in \mathcal{Z}, t \in \mathcal{T}, \quad m \in \mathcal{M}, \quad (12)$$

$$q_{it} \in \{0, 1\} \quad \forall i \in \mathcal{Z}, t \in \mathcal{T}, \quad (13)$$

$$r_{ijt}^m \in \mathbb{R}_0^+ \quad \forall i, j \in \mathcal{Z}, t \in \mathcal{T}, \quad m \in \mathcal{M}, \quad (14)$$

$$s_{it} \in \mathbb{R}_0^+ \quad \forall i \in \mathcal{Z}, t \in \mathcal{T}, \quad (15)$$

$$a_{it} \in \mathbb{R}_0^+ \quad \forall i \in \mathcal{Z}, \quad t \in \{0, 1, \dots, T\}. \quad (16)$$

The objective function (1) maximizes the contribution margin across all periods and results from the rentals at different prices minus the variable costs. Because decisions related to fixed costs cannot be made at this point and are therefore out of scope, maximizing the contribution margin is equivalent to optimizing profit here. Constraints (2) and (3) form the flow conservation that ensure a constant fleet size at all periods. More precisely, (2) connects the available vehicles  $a_{it}$  in location  $i$  at the beginning of period  $t$  to the rentals at all possible prices  $r_{ijt}^m$  that originate at this specific spatio-temporal node plus the vehicles not rented  $s_{it}$ . Constraints (3) determine the available vehicles at the beginning of the next period  $a_{j(t+1)}$  by summing up the arriving rentals and the vehicles not moved. Clearly, (2) and (3) could be formulated in one set of constraints; however, the description of the solution approach in Section 4 becomes more comprehensible with an explicit decision variable  $a_{it}$ . The initial vehicle distribution is set by Constraints (4). Constraints (5) ensure that at every location-time combination only one price  $p^m$  is set.

Constraints (6) and (7) define upper bounds on the rentals, depending on whether demand or supply limits the rentals. For every  $i$ - $j$ - $t$  combination, Constraints (6) limit the rentals observed at a certain price to the actual demand at this price. Additionally, these constraints ensure that only those variables  $r_{ijt}^m$  whose corresponding price  $p^m$  was selected can be positive. Constraints (7) limit the rentals to the number of available vehicles for every location-time combination. More specifically, the rentals from location  $i$  to location  $j$  at period  $t$  and price  $p^m$  must not exceed the fraction  $d_{ijt}^m / \sum_{k \in \mathcal{Z}} d_{ikt}^m \cdot a_{it}$  of available vehicles. The factor  $d_{ijt}^m / \sum_{k \in \mathcal{Z}} d_{ikt}^m$  splits the



available vehicles proportionally into vehicle flows according to the demand relation.

Constraints (8)–(11) are necessary to enforce lower bounds on the rentals, which thereby ensure that if  $p_{it} = p^m$ , rentals realize according to  $r_{it}^m = \min(a_{it}, \sum_{j \in Z} d_{ijt}^m)$  (see *pure pricing* and *proportional demand fulfillment assumptions* in Sections 1 and 3.1; see Soppert et al. (2022) for detailed discussions on *matching functions* that determine  $r_{it}^m$ , including variants to the min-operator applied here). They incorporate a sufficiently large number  $\bar{M}$ . Constraints (8) and (9) force  $q_{it}$  to one if the demand exceeds the available vehicles and to zero otherwise. Now, if demand exceeds the supply, such that  $q_{it} = 1$ , Constraints (11) ensure that all available vehicles are rented. In the other case where  $q_{it} = 0$ , Constraints (10) set the demand as a lower bound for the rentals. As described in the review of the closest related literature in Section 2.3, to the best of our knowledge, none of the existing works on SMS pricing optimization enforces such lower bounds on the rentals. Consequently, these models have a degree of freedom that allows them to reject certain rentals. They therefore do not adequately reflect the real decision problem.

From a technical viewpoint, the OBDPP falls into the class of deterministic sequential decision problems, which are characterized by the fact that they can be divided into stages (Winston and Goldberg 2004, chapter 18.2). In the OBDPP, these stages correspond to the multiple time periods. The corresponding model given in (1)–(16) has the same structure as the general deterministic sequential decision problem stated, for example, in Powell (2011, chapter 4.8.4).

### 3.3. Computational Complexity

**Theorem 1.** *The origin-based differentiated pricing optimization problem in SMSs (OBDPP) (1)–(16) is NP-hard.*

**Proof.** See Online Appendix A.

The proof is performed by polynomial-time reduction of the *three-satisfiability problem* (3-SAT), which is well known to be NP-hard (Garey and Johnson 1990), to the OBDPP. In 3-SAT, multiple *clauses* of three *literals* each build a Boolean *formula*, where the clauses are connected by conjunctions and the literals in each clause by disjunctions, meaning that the formula is in conjunctive normal form (CNF). 3-SAT now asks whether a given 3-CNF formula is *satisfiable*, thus asking whether there exists a consistent *truth assignment* of TRUE/FALSE to the literals, such that the formula is TRUE. The idea of the proof is to construct an OBDPP instance where location-time combinations correspond to a 3-SAT instance's clauses. For each location-time combination, the price selection corresponds to the selection of a literal that is guaranteed

to be TRUE. For the constructed OBDPP instance, determining the optimal solution implies deciding satisfiability of the corresponding 3-SAT instance.

## 4. Approximate Dynamic Programming Decomposition Approach

Given that the OBDPP is NP-hard, in this section, we develop a problem-specific heuristic approach for its solution. More precisely, we propose a decomposition approach based on approximate dynamic programming (ADP). We start by explaining the theoretical foundation of the approach in Section 4.1, followed by its formal description in Section 4.2. In Section 4.3, we describe the specific design of the VFA, which is a central element of the approach. We explain the estimation process of the VFA parameters in Section 4.4.

### 4.1. Theoretical Foundation

The solution approach builds on the general idea of using ADP as a decomposition technique. As Powell (2011) noted, although ADP is known as a solution framework for solving stochastic dynamic decision problems, it can also be applied as a decomposition technique for deterministic sequential decision problems (Powell 2011, chapter 4.8.4), like the OBDPP. Through this technique, multiple smaller problems are solved instead of the original large problem, with each smaller problem containing a VFA that attempts to compensate for the neglected parts of the original problem (Powell 2009, 2016). These VFAs are functions of the decision variables, such that the profits-to-come they approximate are endogenously incorporated within the optimization of the smaller problems. Powell points out that ADP decomposition approaches in principle allow to solve extremely large mathematical programs, which even modern commercial solvers find difficult, but the challenge is to design effective, problem-specific VFAs that yield adequate solution quality.

The ADP decomposition approach we developed for the OBDPP in this study implies a time-based decomposition of the original problem. That is, although in the original problem (1)–(16), all periods  $t \in \mathcal{T}$  are optimized simultaneously, our approach is based on the iterative solution of multiple smaller and adapted versions of the original problem (termed *substitute problem*). More precisely, the approach loops chronologically across all periods  $\tau \in \mathcal{T}$ , and for each  $\tau$ , a substitute problem with fewer explicitly considered periods (termed *horizon*) but with a period-specific VFA at the end of the horizon is optimized.

It is important to note that the ADP decomposition approach goes beyond the basic rolling horizon solution approach for deterministic sequential decision problems, as it is described by Grossmann (2012). In fact, the key idea is to integrate sophisticated VFAs

that allow us to implicitly consider all remaining parts of the original problem that are not considered explicitly in the optimized substitute problem. In our case, these VFAs are functions of the vehicle distribution (decision variables in the substitute problems) such that for *any* resulting vehicle distribution at the end of the horizon, the approximated profit-to-come is endogenously incorporated in the optimization. Thereby, the ADP decomposition approach has an obvious advantage over the basic rolling-horizon approach and comes along with the theoretical potential, in case of perfect VFAs, to indeed find the optimal solution of the overall problem. We describe the details of the approach next.

#### 4.2. Formal Description

We begin the more formal description of the ADP decomposition approach by formalizing the substitute problem at a specific period  $\tau$ . To reduce the problem size, the number of explicitly modeled periods in the substitute problem at period  $\tau$  is limited to the horizon length  $H$  that has to be prespecified. For a certain  $H$ , the explicitly considered periods in the substitute problem at  $\tau$  are the elements of the horizon  $\mathcal{H}_\tau = \{\tau, \tau + 1, \dots, \min(\tau + H - 1, T - 1)\}$ . In other words, this means that periods  $t < \tau$  and  $t > \min(\tau + H - 1, T - 1)$  are not considered explicitly and that the number of periods in the substitute problem can also be fewer than  $H$  in case it would otherwise exceed  $T - 1$ . To compensate for the reduction of explicitly considered periods, the VFA is additionally integrated in the objective function.

To obtain a formulation of the substitute problem on the basis of the original OBDPP (1)–(16), it must be adapted to the considered periods in  $\mathcal{H}_\tau$  and the VFA should be integrated. For that purpose, the decision variable vectors  $\mathbf{y}, \mathbf{q}, \mathbf{r}, \mathbf{a}, \mathbf{s}$  are replaced by  $\tau$ -specific vectors with appropriate time dimension, that is,  $\mathbf{y}_{\mathcal{H}_\tau} = [y_{it}^m]_{Z \times H_\tau \times M}$ ,  $\mathbf{q}_{\mathcal{H}_\tau} = [q_{it}]_{Z \times H_\tau \times M}$ ,  $\mathbf{r}_{\mathcal{H}_\tau} = [r_{ijt}^m]_{Z \times Z \times H_\tau \times M}$ ,  $\mathbf{s}_{\mathcal{H}_\tau} = [s_{it}]_{Z \times H_\tau}$ , where  $H_\tau = \min(H, T - \tau - 1)$ , and  $\mathbf{a}_{\mathcal{H}_\tau} = [a_{it}]_{Z \times (H_\tau + 1) \times M}$ , respectively. For each horizon  $\mathcal{H}_\tau$  with  $\tau \in \mathcal{T}$ , a corresponding substitute problem with initial vehicle distribution  $\hat{\mathbf{a}}_\tau$  is then given by the following MILP:

$$\begin{aligned} & \max_{\substack{\mathbf{y}_{\mathcal{H}_\tau}, \mathbf{q}_{\mathcal{H}_\tau}, \\ \mathbf{r}_{\mathcal{H}_\tau}, \mathbf{a}_{\mathcal{H}_\tau}, \mathbf{s}_{\mathcal{H}_\tau}}}} \sum_{i \in \mathcal{H}_\tau} \sum_{i \in \mathcal{Z}} \sum_{j \in \mathcal{Z}} \sum_{m \in \mathcal{M}} r_{ijt}^m \cdot l_{ij} \cdot (p^m - c) \\ & \quad + \mathbb{1}_{\{\tau+H < T-1\}} \cdot \bar{V}_{\tau+H}(\mathbf{a}_{\tau+H}) \quad (17) \\ \text{s.t.} \quad & \text{Constraints (2)–(3), (5)–(15) with } \mathcal{T} \text{ replaced} \\ & \text{by } \mathcal{H}_\tau, \text{ and (16) with } \{0, 1, \dots, T\} \text{ replaced} \\ & \text{by } \{\tau, \tau + 1, \dots, \min(\tau + H, T)\}, \quad (18) \\ & \text{Constraints (4) with vehicle distribution } \hat{\mathbf{a}}_\tau, \quad (19) \\ & \text{Constraints depending on choice of } \bar{V}_{\tau+H}(\mathbf{a}_{\tau+H}). \quad (20) \end{aligned}$$

Compared with the original OBDPP (1)–(16), the objective function in the substitute problem (17) contains the additional VFA  $\bar{V}_{\tau+H}(\mathbf{a}_{\tau+H})$ . For each substitute problem, the function  $\bar{V}_{\tau+H}(\mathbf{a}_{\tau+H})$  approximates the value at the end of the horizon (i.e., from period  $t = \tau + H$  until the end of the day), referring to the optimal profit-to-come in the original problem for the remaining periods  $\mathcal{R}_{\tau+H} = \{\tau + H, \tau + H + 1, \dots, T - 1\}$ . Because the VFA depends on the vehicle distribution  $\mathbf{a}_{\tau+H} = [a_{i(\tau+H)}]_{Z \times 1}$ , the approximated profit-to-come is endogenously incorporated in the optimization of the substitute problem. More formally, the link between the approximation  $\bar{V}_{\tau+H}(\mathbf{a}_{\tau+H})$  and the original problem for a certain period  $t = \tau + H$  under the respective constraints is

$$\bar{V}_{\tau+H}(\mathbf{a}_{\tau+H}) \approx \max_{\substack{\mathbf{y}_{\mathcal{R}_{\tau+H}}, \mathbf{q}_{\mathcal{R}_{\tau+H}}, \mathbf{r}_{\mathcal{R}_{\tau+H}}, \\ \mathbf{a}_{\mathcal{R}_{\tau+H}}, \mathbf{s}_{\mathcal{R}_{\tau+H}}}} \sum_{t \in \mathcal{R}_{\tau+H}} \sum_{i \in \mathcal{Z}} \sum_{j \in \mathcal{Z}} \sum_{m \in \mathcal{M}} r_{ijt}^m \cdot l_{ij} \cdot (p^m - c), \quad (21)$$

again with adapted vectors of decision variables that now contain the respective variables for all remaining periods  $t \in \mathcal{R}_{\tau+H}$ . The indicator function  $\mathbb{1}_{\{\tau+H < T-1\}}$  in (17) ensures that the VFA is not used beyond the last period of the original problem. We present the details of the VFA design, as well as of determining the function parameters in Section 4.3 and Section 4.4, respectively.

Furthermore, although Constraints (18) in the substitute problem in principle correspond to the original constraints (2)–(3) and (5)–(16), they now account for the new time periods considered explicitly, meaning that  $\mathcal{T}$  is replaced by  $\mathcal{H}_\tau$  and  $\{0, 1, \dots, T\}$  is replaced by  $\{\tau, \tau + 1, \dots, \min(\tau + H, T)\}$ . Likewise, Constraints (19) concerning the substitute problem's initial vehicle distribution remain largely unchanged from (4), but the initial vehicle distribution  $\hat{\mathbf{a}}_\tau = [\hat{a}_{i\tau}]_{Z \times 1}$  at  $\tau$  now is the distribution at the beginning of the substitute problem's horizon. Depending on the specific choice of the VFA  $\bar{V}_{\tau+H}(\mathbf{a}_{\tau+H})$ , additional constraints might be necessary (Constraints (20)). We discuss these regarding our specific VFA design in Section 4.3.

Given the formulation of the substitute problem, we can now solve the original problem using the decomposition approach by chronologically looping over  $\mathcal{T}$ , from  $\tau = 0$  to  $\tau = T - 1$ . In each iteration, we solve a substitute problem (17)–(20) at period  $\tau$  with horizon  $\mathcal{H}_\tau$ . For  $\tau = 0$ , the vehicle distribution is initialized with the vehicle distribution of the original problem  $\hat{\mathbf{a}}_0$ . For all other substitute problems at  $\tau > 0$ , the respective initial vehicle distribution  $\hat{\mathbf{a}}_\tau$  is determined by the vehicle distribution  $\mathbf{a}_\tau$  that realized after one period in the previous substitute problem with horizon  $\mathcal{H}_{\tau-1}$ . The prices  $\mathbf{p}_\tau = [p_{i\tau}]_{Z \times 1}$  that result from the optimization for the first period of each substitute

problem at  $\tau$  are the final prices to be recorded in column  $\tau$  of the price table (Table 1), whereas all other calculated prices are discarded. Similarly, vehicle distributions are computed for the entire horizon, but only the vehicle distribution  $\mathbf{a}_{\tau+1}$  of the next period  $\tau + 1$  is used as initial vehicle distribution  $\hat{\mathbf{a}}_{\tau+1}$  for the next substitute problem. From a technical perspective, already calculated future prices and spatial vehicle distributions can be used as part of a warm start solution in the following substitute problem to speed up the overall solution process.

The general ADP decomposition approach is depicted as pseudo-code in Algorithm 1. The substitute problem including VFA given by (17)–(20) can be solved using a standard mixed-integer programming (MIP) solver. Remember that it is not fully specified yet. We still need to choose a specific VFA to be integrated in Objective (17) and add its corresponding constraints as indicated by (20). We describe our choice of this VFA and the corresponding elements to add in the next section. The computation times for the entire process of pricing solution determination are discussed in Online Appendix D.

**Algorithm 1** (Approximate Dynamic Programming Decomposition Approach)

- start with initial vehicle distribution  $\hat{\mathbf{a}}_0$  according to original problem
- for**  $\tau = 0$  to  $\tau = T - 1$  **do**
- solve substitute problem including VFA (17)–(20) with respective horizon  $\mathcal{H}_\tau$
- store prices  $\mathbf{p}_\tau$  in price table
- update initial vehicle distribution:  $\hat{\mathbf{a}}_{\tau+1} \leftarrow \mathbf{a}_{\tau+1}$
- end for**

### 4.3. Design of the Value Function Approximation

Here we propose and discuss a problem-specific VFA to be used for  $\bar{V}_{\tau+H}$  in (17) and state the additional constraints it requires (cf. (20)). The main focus in our VFA design is to effectively approximate the network effects of the OBDPP. Please remember that the idea is to use the VFA to be able to evaluate *any* vehicle distribution that might arise in the substitute problem.

Basically, the VFA  $\bar{V}_{\tau+H}$  can be any function that maps the decision variables at the end of the horizon to the desired value. In general, three alternative VFA types can be used in ADP: lookup tables, nonparametric value functions, and parametric value functions (Powell 2011, chapter 6). We decided to follow the latter type, that is, a parametric approach, because, different to the others, it can be incorporated in our MILP framework without excessively using auxiliary variables.

The choice of a specific VFA depends on two aspects. First, and most importantly, the VFA should be a good approximation of the true value function

and capture all properties relevant for decision making. The second is tractability. As we integrate the VFA into a MILP, we aim as much as possible to reduce the additional complexity that inevitably results from the VFA integration with its additional decision variables and potential constraints. The first step of the VFA design is known as feature selection in the ADP realm. It determines the variables (a subset of the state) of which the VFA is a function. The vehicle distribution  $\mathbf{a}_{\tau+H}$  is the natural choice, as it is central to the SMS's state, and determines the potential for future rentals. The second step that defines the actual function is a bit more complicated. The key property here is that each additional vehicle in a specific location at time  $\tau + H$  has a positive additional value, but as the number of vehicles increases, the marginal value of each additional available vehicle decreases. This is because the finite demand causes saturation and limits the profit that can be realized with additional vehicles, also taking future demand at other locations through network effects into account. Thus, a concave function seems appropriate. Regarding tractability, linearity in the vehicle distribution  $\mathbf{a}_{\tau+H}$  is desirable.

Combining these arguments and computational tests, we propose a piecewise linear function of the number of vehicles in each location at time  $\tau + H$ . Additional constraints ensure concavity. Thus, the VFA captures the decreasing marginal value of available vehicles and retains linearity. In particular, the VFA (incorporated in the substitute problem (17)–(20)) is the following  $Z$ -dimensional piecewise linear function with  $K$  pieces in each dimension.

$$\bar{V}_{\tau+H}(\mathbf{a}_{\tau+H}) := \sum_{i \in \mathcal{Z}} \sum_{k \in \mathcal{K}} \bar{v}_{i(\tau+H)}^k \cdot \Delta a_{i(\tau+H)}^k + \bar{v}_{\tau+H}^{\text{const}} \quad (22)$$

Technically speaking, the VFA (22) for a specific period  $\tau + H$  is a function of the respective spatial vehicle distribution  $\mathbf{a}_{\tau+H}$  and additive over the  $Z$  locations. For a specific location  $i$ , the present vehicles  $a_{i(\tau+H)}$  are divided into  $K$  buckets that each represent a common marginal value per vehicle and correspond to the pieces of the piecewise linear function. The number of vehicles in these buckets is modeled by additional decision variables  $\Delta a_{i(\tau+H)}^k$  (= pieces) with  $a_{i(\tau+H)} = \sum_{k \in \mathcal{K}} \Delta a_{i(\tau+H)}^k \quad \forall i \in \mathcal{Z}$ , where  $\mathcal{K} = \{1, \dots, K\}$ . Thus, a specific share  $\Delta a_{i(\tau+H)}^k$  of the vehicles at location  $i$ , period  $(\tau + H)$  now corresponds to piece  $k$  and contributes with the respective marginal value  $\bar{v}_{i(\tau+H)}^k$  to the overall value of the VFA. Additionally, the VFA contains the time specific constant  $\bar{v}_{\tau+H}^{\text{const}}$ .

The VFA parameters, meaning  $\bar{v}_{i(\tau+H)}^k$  for  $i \in \mathcal{Z}, \tau + H \in \mathcal{T}, k \in \mathcal{K}$ , as well as  $\bar{v}_{\tau+H}^{\text{const}}$  for  $(\tau + H) \in \mathcal{T}$ , are derived in an estimation process that we describe in Section 4.4. Because of the decreasing marginal value

of vehicles discussed previously, during estimation, we enforce concavity of the function in each dimension  $i$  by requiring  $\bar{v}_{i(\tau+H)}^k \geq \bar{v}_{i(\tau+H)}^{k+1} \forall i \in \mathcal{Z}$  and  $\forall k \in \{1, \dots, K-1\}$ . Furthermore, we require  $\bar{v}_{i(\tau+H)}^k \geq 0 \forall i \in \mathcal{Z}$ ,  $k \in \mathcal{K}$  and  $\bar{v}_{\tau+H}^{const} \geq 0$  for obvious reasons.

As a side note, for an efficient VFA of our problem, considering  $i$ - $t$ -specific parameters  $\bar{v}_{i(\tau+H)}^k$  is indeed decisive. The intuition behind this is that a vehicle's value depends on both location and time. In particular, parameters that were only time-specific would result in a valuation of the fleet at the end of the horizon which is identical for all possible fleet distributions.

Now, to plug the VFA (22) into the substitute problem (17)–(20) for period  $\tau$  with horizon  $\mathcal{H}_\tau$ , we obviously substitute (22) into the objective function (17). Moreover, additional continuous and nonnegative decision variables  $\Delta a_{i(\tau+H)}^k \forall i \in \mathcal{Z}, k \in \mathcal{K}$  are introduced. To ensure a correct evaluation of the vehicle distribution  $\mathbf{a}_{\tau+H}$  with (22), the following additional constraints need to be integrated in the substitute problem for (20):

$$a_{i(\tau+H)} = \sum_{k \in \mathcal{K}} \Delta a_{i(\tau+H)}^k \quad \forall i \in \mathcal{Z} \quad (20a)$$

$$\Delta a_{i(\tau+H)}^k \leq \Delta \tilde{a} \quad \forall i \in \mathcal{Z}, \forall k \in \{1, 2, \dots, K-1\}. \quad (20b)$$

Constraints (20a) ensure that the  $\Delta a_{i(\tau+H)}^k$  indeed sum up to the vehicle count. By Constraints (20b), the number of vehicles in each bucket, except for the last bucket ( $\Delta a_{i(\tau+H)}^K$ ), is limited to the respective predefined bucket size  $\Delta \tilde{a}$ . Because of the concavity of the VFA, the buckets are “automatically” filled in the correct order, beginning with  $k = 1$ .

To solve the substitute problem (17)–(20) incorporating this VFA, we still need values for its parameters. We describe their estimation in the next section.

#### 4.4. Parameter Estimation

The estimation process we propose for the VFA parameters is performed before we loop over the time periods and iteratively solve the substitute problems as described in Sections 4.1 and 4.2. We followed the traditional idea of parameter estimation based on observed data, which, in our case, is artificial sample data generated from simulations, as common in ADP-based approaches. For the purpose of sample generation, we exploit that for a given spatial vehicle distribution at a certain period and with a given price table for the remaining periods, the resulting rentals of the remaining periods and thus the corresponding profit-to-come are easily calculated algorithmically. This profit-to-come evaluation is computationally efficient, even for real-life instances. The overall process can roughly be outlined as follows: First, we generate samples of vehicle distributions. Second, for each sample, we calculate the resulting profit-to-come. Finally, these data are used to estimate

the VFA parameters by an adapted least squares estimation procedure.

More formally, for each period  $(\tau + H) \in \{1, 2, \dots, T-1\}$ , multiple samples  $n \in \mathcal{N} = \{1, 2, \dots, N\}$  of vehicle distributions  $\hat{\mathbf{a}}_{\tau+H}^n = [\hat{a}_{i(\tau+H)}^n]_{\mathcal{Z} \times 1}$  are drawn by randomly splitting up the fleet among the  $Z$  locations. For each of these vehicle distribution samples  $\hat{\mathbf{a}}_{\tau+H}^n$ , a corresponding profit-to-come  $\hat{V}_{\tau+H}^n(\hat{\mathbf{a}}_{\tau+H}^n)$  is determined by evaluating a known (suboptimal) price table; for example, one that only consists of a constant uniform price, over the remaining periods. This could be done by applying a solver to evaluate the original problem (1)–(16) with fixed prices for the remaining periods in  $\mathcal{R}_{\tau+H}$ , but an equivalent algorithmic solution is straightforward and much faster. Moreover, for each vehicle distribution the number of vehicles in each bucket,  $\Delta \hat{\mathbf{a}}_{\tau+H}^n = [\Delta \hat{a}_{i(\tau+H)}^{k,n}]_{\mathcal{Z} \times 1 \times \mathcal{K} \times N}$  is calculated. In particular, for each location, we simply assign as many vehicles as possible up to the bucket size  $\Delta \hat{a}_{i(\tau+H)}^{k,n}$  to a bucket and then continue with the next with increased  $k$ .

Given the resulting sample data, the respective parameters  $\bar{\mathbf{v}}_{\tau+H} = [\bar{v}_{i(\tau+H)}^k]_{\mathcal{Z} \times 1 \times \mathcal{K}}$  and  $\bar{v}_{\tau+H}^{const}$  from the VFA (22) are simultaneously determined by constrained least squares estimation, that is, a variant of ordinary least squares estimation with additional equality and inequality constraints. More precisely, we minimize the mean squared error over the  $N$ -generated data points by the following quadratic optimization problem:

$$\min_{\bar{\mathbf{v}}_{\tau+H}, \bar{v}_{\tau+H}^{const}} \frac{1}{N} \sum_{n \in \mathcal{N}} (\hat{V}_{\tau+H}^n(\hat{\mathbf{a}}_{\tau+H}^n) - \bar{V}_{\tau+H}^n(\Delta \hat{\mathbf{a}}_{i(\tau+H)}^n))^2 \quad (23)$$

$$\text{s.t. } \bar{V}_{\tau+H}^n(\Delta \hat{\mathbf{a}}_{i(\tau+H)}^n) = \sum_{i \in \mathcal{Z}} \sum_{k \in \mathcal{K}} \bar{v}_{i(\tau+H)}^k \cdot \Delta \hat{a}_{i(\tau+H)}^{k,n} + \bar{v}_{\tau+H}^{const} \quad \forall n \in \mathcal{N}, \quad (24)$$

$$\bar{v}_{i(\tau+H)}^k \geq 0 \quad \forall i \in \mathcal{Z}, k \in \mathcal{K}, \quad (25)$$

$$\bar{v}_{\tau+H}^{const} \geq 0, \quad (26)$$

$$\bar{v}_{i(\tau+H)}^k \geq \bar{v}_{i(\tau+H)}^{k+1} \quad \forall i \in \mathcal{Z}, \quad k \in \{1, 2, \dots, K-1\}. \quad (27)$$

The error minimized in (23) is the mean of the squared difference between the observed (evaluated) profits-to-come  $\hat{V}_{\tau+H}^n$  and the profits-to-come  $\bar{V}_{\tau+H}^n$  predicted with (22) (identical to (24)), for the respective observed (randomly drawn) spatial vehicle distribution, over all samples  $N$ . Constraints (25)–(26) ensure the nonnegativity of the parameters, and Constraints (27) ensure the VFA's concavity. Remember that  $\bar{\mathbf{v}}_{\tau+H}$  and  $\bar{v}_{\tau+H}^{const}$  are parameters in their eventual use as parts of the VFA in the substitute problem (17)–(20), but here in (23)–(27), they are the decision variables to be determined.

The parameter estimation is performed individually for each period  $(\tau + H) \in \mathcal{T}$  but simultaneously over

all  $Z$  locations each  $(\tau + H)$  such that spatio-temporal interdependencies are captured by the VFA parameters. The process is depicted as pseudo-code in Algorithm 2. We solve (23)–(27) using a standard MIP solver. Computation times for the parameter estimation process are discussed in Online Appendix D.

**Algorithm 2** (Parameter Estimation Algorithm)

```

for  $(\tau + H) = 1$  to  $T - 1$  do
  for  $n = 1$  to  $N$  do
    – randomly divide fleet into spatial vehicle distribution  $\hat{\mathbf{a}}_{\tau+H}^n$ 
    – determine profit-to-come  $\hat{V}_{\tau+H}^n$  by algorithmic evaluation of original problem (1)–(16) for remaining periods  $\mathcal{R}_{\tau+H}$  with known (suboptimal) price solution
    – for each location, calculate number of vehicles in each bucket ( $\Delta \hat{\mathbf{a}}_{\tau+H}^n$ )
  end for
  – determine VFA parameters  $\bar{\mathbf{v}}_{\tau+H}$  and  $\bar{v}_{\tau+H}^{const}$  by (23)–(27)
end for

```

## 5. Computational Experiments

We investigate the performance of the ADP decomposition approach presented in Section 4 in comprehensive computational experiments. We vary the most relevant influencing factors systematically to triangulate the approach's performance. Section 5.1 introduces the scenarios and parameter values. In Section 5.2, we state all solution approaches that we investigate, including benchmarks, as well as the metrics we use for their evaluation. In Section 5.3, we present and discuss the computational results.

### 5.1. Scenarios and Parameters

We consider three *settings* of a free-floating SMS that primarily differ in the number of zones (= locations),  $Z = 9$ ,  $Z = 16$ , and  $Z = 25$ , but also regarding the demand pattern. The process used to generate the base demand matrix  $\mathbf{d}$  with values for all zone-zone-period combinations allows to incorporate typical demand characteristics that we observed in practice, namely a typical demand pattern over the course of the day and differentiation between zone types, like city center zones or peripheral zones (Reiss and Bogenberger 2016). The exact procedure is explained in Online Appendix B. The remaining parameters are constant over all three settings: we discretize the time interval of one day into  $T = 48$  periods of 30 minutes each, in line with practice and literature (Ferrero et al. 2015b, Kaspi et al. 2016). The parameters  $\hat{a}_{i,0} = 2 \forall i \in \mathcal{Z}$  represent a realistic number of vehicles per zone. We select the  $M = 3$  price points  $p^m$  according to typical prices in practice and literature (Lippoldt, Niels, and Bogenberger 2018): we choose a base price of  $p^{(2)} = 30$  ct/min and price differences of 20% to the

low and high price, such that  $p^{(1)} = 24$  ct/min and  $p^{(3)} = 36$  ct/min. The corresponding sensitivity factors  $f_{ijt}^{(1)} = 1.25, f_{ijt}^{(2)} = 1, f_{ijt}^{(3)} = 0.75 \forall i, j \in \mathcal{Z}, t \in \mathcal{T}$  are chosen according to observations from practice. Variable costs of  $c = 7.5$  ct/min made up 25% of the base price. The average rental time was set to  $l_{ij} = 15$  minutes  $\forall i, j \in \mathcal{Z}$ , again in line with literature (Xu, Meng, and Liu 2018) and after discussions with our practice partner.

To generate different *scenarios* within a *setting*, the overall demand level can be adjusted by the *demand-supply-ratio*  $\delta$ , which determines the ratio of the maximum period demand during the day  $\bar{d}$  and the fleet size  $\sum_{i \in \mathcal{Z}} \hat{a}_{i,0}$ . Although the fleet size remains constant for all *scenarios* within a *setting*, the overall demand varies according to  $\delta$ , that is,  $\bar{d} = \sum_{i \in \mathcal{Z}} \hat{a}_{i,0} \cdot \delta$ . The required (base) demand of a scenario for every location-location-period combination  $d_{ijt}$  is then simply determined by scaling  $\bar{d}$  according to the given demand pattern, which is defined by *ratios* of the  $d_{ijt}$  among one another. As a result,  $\bar{d} = \max_t (\sum_{i,j \in \mathcal{Z}} d_{ijt})$  holds. We use demand patterns that replicate typical spatio-temporal differences, for example, that show the two characteristic demand peaks over the course of a day, as observed in practice by our practice partner. This is typical for SMSs and has been similarly reported in many other studies, such as Reiss and Bogenberger (2016). Although the maximum period demand only reflects the demand of a single period, it is a representative, yet simple, metric for the overall demand, because all SMSs in practice show a comparable course of demand across the day. The demand-supply-ratios we use are  $\delta \in \{2/6, 4/6, 6/6, 8/6\}$ . Furthermore, as already mentioned, each combination of a certain *setting* with a specific  $\delta$  forms a *scenario*.

### 5.2. Investigated Solution Approaches and Evaluation Metrics

Here, we describe the *solution approaches* that we investigate. Besides our ADP decomposition approach with three different configurations, we investigate four benchmark approaches, of which one again has three *configurations* (the approaches are summarized in Table 2):

- ADP-H is the ADP decomposition solution approach we presented in Section 4 and is configured with different horizon lengths  $H$  (ADP-1, ADP-4, ADP-8).
- CUP denotes a lower benchmark using constant uniform pricing. Because of its wide adoption over all SMS types, this pricing can be considered as the de facto standard applied in practice. Here we used the base price  $p_{it} = p^{(2)}$  for all  $i \in \mathcal{Z}$  and  $t \in \mathcal{T}$ .
- OPT denotes the optimal solution of the OBDPP in which all 48 periods are optimized simultaneously. It provides an upper bound. This benchmark can be calculated for some of the scenarios.

**Table 2.** Overview of Solution Approaches Investigated

	Description	Configurations
ADP-H	ADP decomposition approach with horizon length $H$	ADP-1, ADP-4, ADP-8
CUP	Benchmark: constant uniform pricing	—
OPT	Benchmark: optimal pricing	—
UB	Benchmark: best upper bound after a computation time limit	—
ROL-H	Benchmark: rolling-horizon approach with horizon length $H$	ROL-1, ROL-4, ROL-8

• UB denotes the best known upper bound that the solver returned after a computation time limit.

• ROL-H is a basic rolling-horizon approach. In the context of our work, it is best described as a variant of the ADP decomposition approach without the VFA at the end of the horizon, that is,  $\bar{V}_{\tau+H} = 0 \forall (\tau + H) \in \mathcal{T}$ . We considered this benchmark to analyze the impact of the VFA in our approach. Like ADP-H, it can be configured for different horizon lengths  $H$  (ROL-1, ROL-4, ROL-8). This benchmark with  $H = 1$  represents the myopic solution that only considers one period in each substitute problem without anticipating any network effects.

Each combination of scenario and solution approach configuration forms a *test instance* in our experiments. Table 7 in Online Appendix C summarizes the test instances that we evaluate.

Regarding the VFA, we define the parameters that specify the structure of the function and the estimation process as follows. The number of buckets (pieces) is  $K = 10$ , and the bucket size is  $\Delta\bar{a} = 2$ . For each scenario, we perform the parameter estimation as described in Section 4.4 on  $n = 10,000$  samples. In each period  $(\tau + H) \in \mathcal{T}$ , we randomly generate the initial vehicle distribution  $\hat{\mathbf{a}}_{\tau+H}^n$  following the Dirichlet distribution and use the CUP solution for evaluating the original problem (1)–(16) for the remaining periods in  $\mathcal{R}_{\tau+h}$  to obtain  $\hat{V}^n(\hat{\mathbf{a}}_{\tau+H}^n)$ .

We use various *metrics* to evaluate the solution approaches and to discuss further insights. We describe these metrics in the following exposition. We summarize them in Table 3, as well as formally define them in Table 8 in Online Appendix C. Profit ( $PR_{(\cdot)}^{rel}$ ), revenue ( $RV_{(\cdot)}^{rel}$ ), and rentals ( $RT_{(\cdot)}^{rel}$ ) are stated as relative improvements to the respective value from the uniform pricing solution. Depending on the analysis, we consider the overall improvements across all

periods  $t \in \mathcal{T}$  (e.g.,  $PR^{rel}$ ) or one particular period  $t$  (e.g.,  $PR_t^{rel}$ ). Furthermore, we consider the proportion of location-time combinations in which a particular price  $p^m$  is selected ( $P_{(\cdot)}^{prop}$ ) and the proportion of rentals that occur at price  $p^m$  ( $RT_{(\cdot)}^{prop}$ ) for all periods  $t \in \mathcal{T}$  ( $P_{p^m}^{prop}, RT_{p^m}^{prop}$ ) and for a specific period  $t$  ( $P_{p^m t}^{prop}, RT_{p^m t}^{prop}$ ).

We implement the algorithms in Python 3.7 and solve all MILPs with Gurobi 9.0.2. In all scenarios with nine zones, we set the target optimality gap to zero in Gurobi and no time limit in any of the approaches is imposed. In all scenarios with 16 and 25 zones, the time limit is set at one hour for the substitute problems of the ADP-H and ROL-H approaches and at 48 hours for UB. Additionally, we use the CUP solution as a warm start solution in all instances. We execute our computations on a workstation with two Intel Xeon E7-8890 v3 2.5 GHz processors with a total of 36 cores, and 512 GB RAM.

### 5.3. Results

In the following sections, we present and discuss our computational results. First, we determine how much improvement is possible beyond myopic pricing (ROL-1; Section 5.3.1). Next, we investigate how much of this potential can be realized with the ADP-H and ROL-H approaches (Section 5.3.2) and in this context we show the importance of the VFA by comparing ADP-H to ROL-H. Then, we discuss the impact of accounting for network effects on the pricing (Section 5.3.3) and intuitively illustrate how the VFA captures network effects, as well as the future value of available vehicles (Section 5.3.4). Finally, we analyze the robustness of the results by considering a stochastic environment (Section 5.3.5).

We discuss the results for all demand-supply ratios  $\delta$  here but depict only those of the profit for  $\delta = 2/6$ , illustratively. All other results are depicted in Online

**Table 3.** Evaluation Metrics

	Description	Variant
$PR^{rel}$	Relative profit increase w.r.t. CUP	Time specific: $PR_t^{rel}$
$RV^{rel}$	Relative revenue increase w.r.t. CUP	Time specific: $RV_t^{rel}$
$RT^{rel}$	Relative rentals increase w.r.t. CUP	Time specific: $RT_t^{rel}$
$P_{p^m}^{prop}$	Proportion of price $p^m$ in pricing solution	Time specific: $P_{p^m}^{prop}$
$RT_{p^m}^{prop}$	Proportion of rentals at price $p^m$ in pricing solution	Time specific: $RT_{p^m}^{prop}$

Appendices E (9-zone setting) and F (16- and 25-zones settings). Computation times are discussed in Online Appendix D.

**5.3.1. Improvement Potential over Myopic Pricing.** We begin by identifying the improvement potential over myopic pricing, that is, the relative difference in profit  $PR^{rel}$  between the myopic (ROL-1) and upper benchmarks. For the nine-zones setting, we use the optimal (OPT) solution as upper benchmark. For the 16- and 25-zones setting, the optimal solution cannot be determined in reasonable time; therefore, we use the best known upper bound (UB) as benchmark. The idea is that the range between the lower and upper benchmarks is an upper bound on the potential of  $PR^{rel}$  that can be achieved by the ADP decomposition approach. We consider the latter approach in Section 5.3.2.

This potential is graphically given in Figure 2. It depicts the profit obtained with the different solution approaches (in dependence of the horizon length  $H$  for ADP-H and ROL-H, see Section 5.3.2) relative to the profit with CUP, which the 0% line marks. The profits obtained by OPT and UB are horizontal lines because they do not depend on  $H$ . We observe that OPT and UB yield a profit increase of about 15% over CUP. The myopic solution ROL-1 provides about 5% more profit than CUP. Thus, the potential improvement over myopic pricing is about 10 percentage points. We return to Figure 2 in the following section to discuss the other results included.

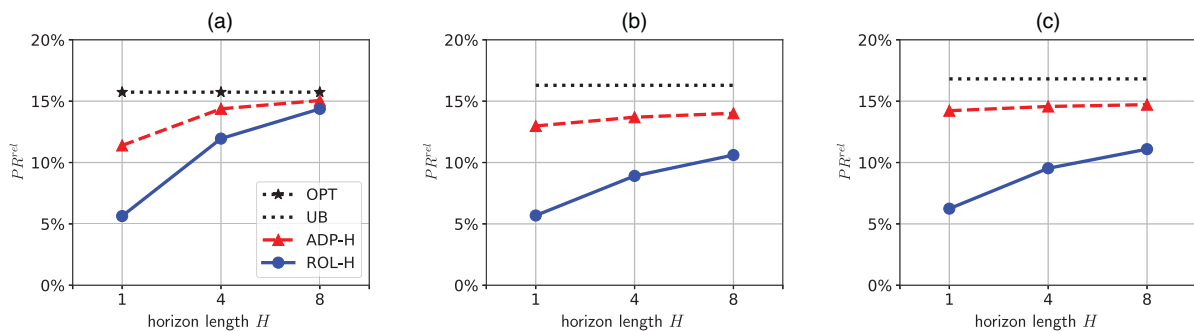
Figure 14 in Online Appendix E depicts the results for all scenarios with  $\delta$  from 2/6 to 8/6 (rows) in the nine-zones setting. The potential for improvement between ROL-1 and OPT decreases from 10.1 percentage points for  $\delta = 2/6$  to 2.3 percentage points for  $\delta = 8/6$ . The scenarios with  $\delta < 6/6$  are especially relevant for practice (Section 6.1). These results are also valid for the 16- and 25-zones settings (see Figure 15 in Online Appendix F).

What makes the difference between the scenarios is obviously the relevance of network effect anticipation, because ROL-1 considers only one period in each substitute problem and includes no VFA and therefore no network effects. The intuition is that in high-demand scenarios (large  $\delta$ ), there is almost always demand for an available vehicle, because the demand is never the limiting factor. In low-demand scenarios, however, vehicles remain unused more often. This conclusion is supported by the comparison of rentals ( $RT^{rel}$ ) in the third column of Figure 14, which shows a substantial difference of 3.8 percentage points between ROL-1 and OPT for  $\delta = 2/6$  and almost no difference for  $\delta = 8/6$ .

### 5.3.2. Performance of the ADP Decomposition Approach.

After identifying the potential of up to 10 percentage points for improvement over the myopic solution ROL-1, we now analyze the performance of the proposed ADP decomposition approach (ADP-H). To do so, we revisit Figure 2(a) and consider the profit  $PR^{rel}$  of ADP-1, ADP-4, and ADP-8. In the nine-zones setting, we observe that as the horizon length  $H$  increases,  $PR^{rel}$  increases from 11.4% (ADP-1) to 15.1% (ADP-8). Additionally, the improvement potential identified in Section 5.3.1 is almost entirely exploited. The results for the 16- and 25-zones settings are similar. An additional profit increase does not necessarily go hand in hand with a revenue  $RV^{rel}$  and rentals  $RT^{rel}$  increase, as depicted for the nine-zones setting in the second and third columns of Figure 14 in Online Appendix E. Sometimes profit increases because of a quantity effect when the differentiated pricing enables more rentals while the average price remains more or less constant. The underlying reason is a better positioning of vehicles because of the network effect consideration. At other times, profit increases because of a price effect at rather constant rentals with increase average price or even at fewer rentals when the average price decreases underproportionally.

**Figure 2.** (Color online) Relative Profit Increase in Settings with 9, 16, and 25 Zones



Notes. Demand-supply-ratio  $\delta = 2/6$ . (a)  $Z = 9$ . (b)  $Z = 16$ . (c)  $Z = 25$ .

Again referring to Figure 2(a), we see that the integrated VFA in ADP-1 and ADP-4 has a substantial benefit of 5.8 and 2.4 percentage points over their ROL-H counterparts. For ROL-8/ADP-8, the benefit is smaller. For smaller horizon lengths, the potential for improvement by the VFA is obviously higher than for larger horizon lengths because both the explicit consideration of additional periods in a longer horizon and the VFA aim to consider the spatio-temporal network effects. As settings become larger, the benefit of ADP-H over ROL-H increases, and with 16- and 25-zones even ADP-1 performs considerably better than the ROL-8 benchmark procedure (Figure 2, (b) and (c)).

The results for all scenarios in the 9-zones setting (Figure 14, Online Appendix E) and all scenarios in the 16- and 25-zones settings (Figure 15, Online Appendix F) confirm the findings discussed previously. Most importantly, the profits obtained with ADP-H are at least as high as the respective variant of ROL-H, but especially for the practice-relevant scenarios with low  $\delta$ , there is substantial improvement. This demonstrates that integrating the VFAs can partly compensate for not considering all spatio-temporal network effects explicitly. The fewer network effects are captured within the horizon, the stronger the effect.

Another benefit of the ADP decomposition approach concerns its scalability to large problem instances. As preliminary studies have shown, problem complexity (NP-hardness of the OBDPP) takes its toll, and finding good solutions in reasonable time cannot be guaranteed. By contrast, ADP-H benefits from the decomposition and can therefore cope with the larger problem size while simultaneously considering network effects.

**5.3.3. Investigation of Pricing.** The differences in considering network effects of the myopic (ROL-1) and the optimal solution (OPT) identified in Section 5.3.1 are also reflected in the pricing decisions, depicted as

price tables in Figure 3, (a) and (b), for the nine-zones setting with  $\delta = 2/6$ . On an aggregate level, these differences become obvious in comparing the proportions of the ROL-1 and OPT prices  $PR^{prop}$  in the fourth column of Figure 14 in Online Appendix E. For  $\delta = 2/6$ , for example, the ROL-1 solution consists of 1.6% low, 76.9% base, and 21.5% high prices. The OPT solution consists of 34.5% low, 28.7% base, and 36.8% high prices.

The better network effects are captured, the more the resulting pricing decisions resemble the optimal pricing, as the price tables for ADP-1 and ADP-8 depicted in Figure 3 (c) and (d), demonstrate. Especially the difference between ROL-1 and ADP-1 is insightful. Again, the aggregate price proportions  $P_{p^m}^{prop}$  which are depicted in Figure 14 (Online Appendix E) and Figure 15 (Online Appendix F) underline how the network effect integration, especially with ADP-H, affects the pricing.

**5.3.4. Investigation of the Value Function Approximation.**

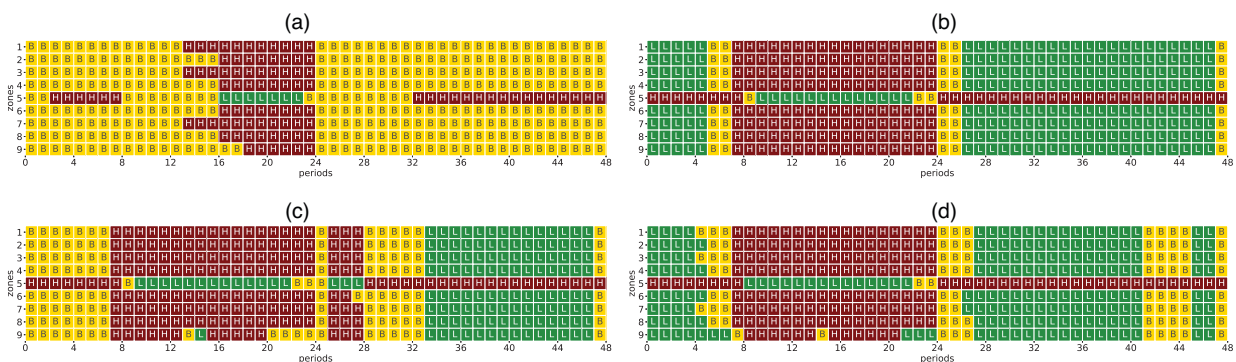
Integrating the VFA that captures the spatio-temporal network effects beyond the explicitly considered horizon’s end is an integral component of the ADP decomposition approach. In this section, we illustrate how the VFA works and illustratively interpret the estimated values we obtained. In particular, the following analyses demonstrate how the VFA’s parameters reflect the demand pattern and thus capture short-term and long-term vehicle values. For ease of readability, we first repeat the VFA given in Section 4.3:

$$\bar{V}_{\tau+H}(\mathbf{a}_{\tau+H}) = \sum_{i \in \mathcal{Z}} \sum_{k \in \mathcal{K}} \bar{v}_{i(\tau+H)}^k \cdot \Delta a_{i(\tau+H)}^k + \bar{v}_{\tau+H}^{const} \quad (28)$$

For the sake of clearer analyses, we define its zone-specific parts as

$$\bar{V}_{i(\tau+H)}^{part}(a_{i(\tau+H)}) = \sum_{k \in \mathcal{K}} \bar{v}_{i(\tau+H)}^k \cdot \Delta a_{i(\tau+H)}^k \quad (29)$$

Figure 3. (Color online) Pricing with Different Solution Approaches in Nine-Zones Setting



Notes. Demand-supply-ratio  $\delta = 2/6$ . B, base price; H, high price; L, low price. (a) ROL-1. (b) OPT. (c) ADP-1. (d) ADP-8.



**Table 4.** Parameter Estimates of VFA for Two Exemplary Periods and Zones

Period	Zone	$\bar{v}_{i(\tau+H)}^k$										$\bar{v}_{\tau+H}^{const}$
		$k = 1$	$k = 2$	$k = 3$	$k = 4$	$k = 5$	$k = 6$	$k = 7$	$k = 8$	$k = 9$	$k = 10$	
$(\tau + H) = 16$	$i = 1$	9.79	2.30	1.54	1.54	1.42	1.27	0.00	0.00	0.00	0.00	140.63
	$i = 5$	6.45	5.82	5.82	5.66	5.44	5.44	5.22	3.49	0.00	0.00	
$(\tau + H) = 32$	$i = 1$	3.31	3.25	3.25	3.25	3.25	3.25	3.25	0.00	0.00	0.00	1.36
	$i = 5$	7.33	7.28	7.17	7.06	6.96	6.85	6.85	0.00	0.00	0.00	

such that

$$\bar{V}_{\tau+H}(\mathbf{a}_{\tau+H}) = \sum_{i \in Z} \bar{V}_{i(\tau+H)}^{part}(\mathbf{a}_{i(\tau+H)}) + \bar{v}_{\tau+H}^{const} \quad (30)$$

Table 4 contains an extract of the slope parameters  $\bar{v}_{i(\tau+H)}^k$  and the constants  $\bar{v}_{\tau+H}^{const}$  for two periods ( $(\tau + H) = 16$  at morning peak time and  $(\tau + H) = 32$  at evening peak time) and two zones (center zone  $i = 5$  and peripheral zone  $i = 1$ ). The values result from the estimation process of the scenario with  $Z = 9$  zones and demand-supply-ratio  $\delta = 2/6$ . The biggest absolute difference between the respective parameters concerns the constants with  $\bar{v}_{16}^{const} = 140.63$  and  $\bar{v}_{32}^{const} = 1.36$ . As the value function  $\bar{V}_{\tau+H}$  approximates the profit-to-come from a certain period  $(\tau + H)$  onwards, the difference in the constants reflects the higher demand-to-come at an earlier time. This time dependence of  $\bar{v}_{\tau+H}^{const}$  is also visible in Figure 4. The close connection to the demand-to-come is obvious from comparing its course over the day, as depicted in Figure 5.

The slope parameters  $\bar{v}_{i(\tau+H)}^k$  during the evening peak period  $(\tau + H) = 32$  take larger values for the center zone  $i = 5$  than for the peripheral zone  $i = 1$ , reflecting that vehicles in the center have a higher value. This is because demand in the center zone is higher during the evening peak. This is reflected in the VFA by the parts  $\bar{V}_{1,32}(a_{1,32})$  and  $\bar{V}_{5,32}(a_{5,32})$  for zones 1 and 5, which are depicted in Figure 6(b). Both curves, the solid one representing the value in zone  $i = 1$  and the dashed one for zone  $i = 5$ , are concave with a positive slope in the origin and a saturation with zero

slope from a certain vehicle count  $a_{it}$  onward. Concavity and saturation represent the diminishing marginal value of additional vehicles and the assumptions imposed in the estimation process.

During the morning peak period at  $(\tau + H) = 16$ , the zone-specific VFAs  $\bar{V}_{i16}(a_{i16})$  for the same two zones  $i = 1$  and  $i = 5$  are depicted in Figure 6(a). There is also concavity and saturation, but the functions intersect. As the slope parameters in Table 4 show, the first slope parameter for zone 1 takes higher values than the corresponding values of zone 5, meaning  $\bar{v}_{1,16}^k > \bar{v}_{5,16}^k$  for  $k = 1$ . For  $k > 1$ , however, the order of slope values switches, such that  $\bar{v}_{1,16}^k \leq \bar{v}_{5,16}^k$ . These parameters and the resulting curves can be explained by analyzing the demand. Figure 6(c) shows that at  $(\tau + H) = 16$ , the demand of zone 1 is slightly higher than that of zone 5. The demand-to-come from  $(\tau + H) = 16$  on in zone 5, however, is much higher, as Figure 6(d) displays. Because the demand after the morning peak in zone 1 is low, putting more than two vehicles in that zone will not deliver high value, and for more than 12 vehicles zero additional value will accrue. In contrast, the higher demand-to-come in zone 5 will lead to a positive value for additional vehicles, which explains the later saturation of  $\bar{V}_{5,16}(a_{5,16})$  at higher vehicle count  $a_{5,16}$ . This shows how the VFA reflects short-term and long-term network effects because of temporal demand variations. The magnitudes of the  $\bar{v}_{i(\tau+H)}^k$  values and  $\bar{v}_{\tau+H}^{const}$  values (with an average of two vehicles per zone) in Table 4 indicate that they both represent decisive VFA features.

**Figure 4.** (Color online) Value of the Constant  $\bar{v}_t^{const}$  in the VFA

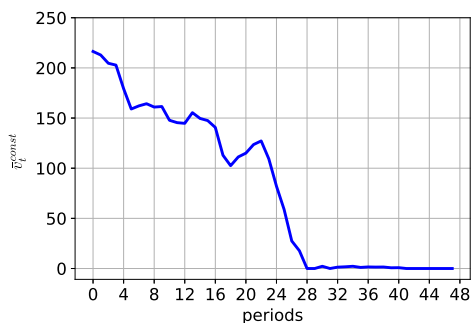


**Figure 5.** (Color online) Base Demand-to-Come

$$\sum_{\tau=t}^{T-1} \sum_{i,j \in Z} d_{ij\tau}$$

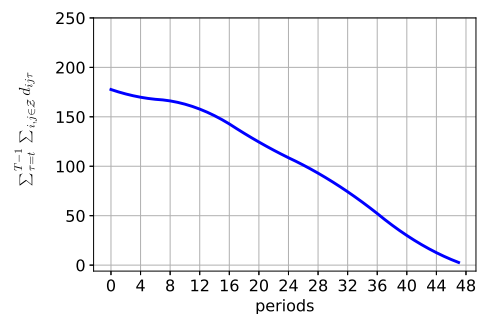
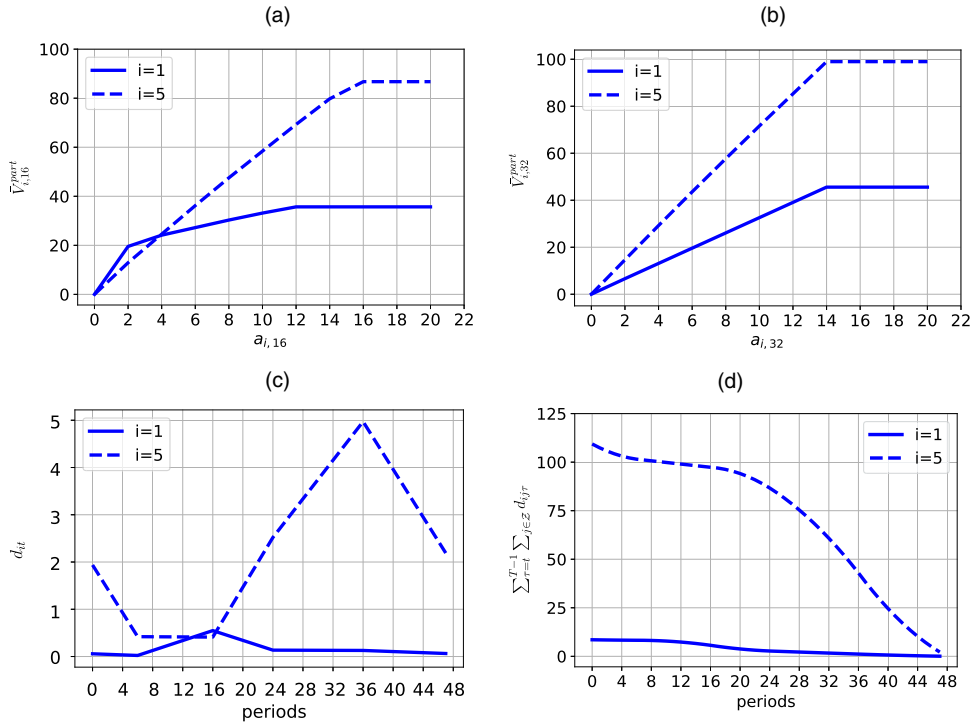


**Figure 6.** (Color online) Parts of the VFA for Two Selected Zones at Periods 16 (a) and 32 (b), Base Demand (c), and Cumulated Base Demand (d) over the Course of the Day



**5.3.5. Stochastic Demand.** To analyze the robustness of the results, we additionally evaluate the pricing resulting from different solution approaches in a stochastic environment. For this purpose, we apply a *multiplicative stochastic demand function*, which is one of the standard approaches of modeling demand as described, for example, in Talluri and van Ryzin (2004, chapter 7.3.4). More precisely, base demand is now a random variable  $D_{ijt}$  with

$$D_{ijt} = \xi \cdot d_{ijt}, \quad (31)$$

where  $\xi$  is a stochastic error term that is assumed to follow a normal distribution  $\mathcal{N}(1, \sigma^2)$ .

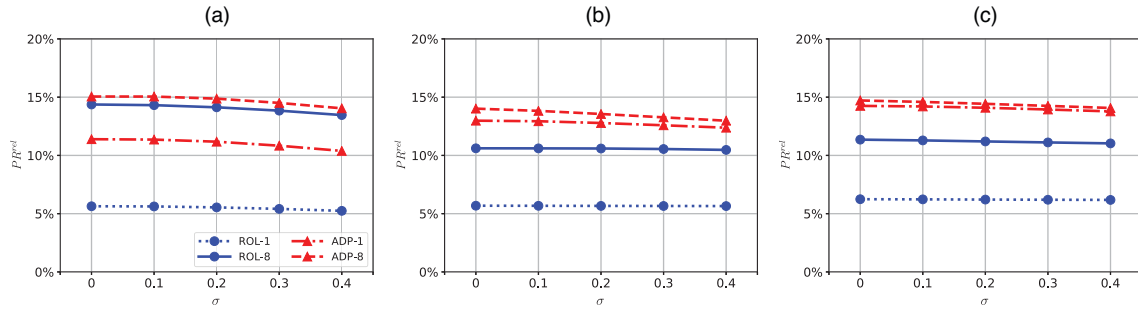
Based on this demand model, we evaluate all scenarios from Section 5.1, that is, the 9-, 16-, and 25-zones settings with all demand-supply-ratios  $\delta$ . For each scenario, we consider different degrees of stochasticity, expressed by different standard deviations  $\sigma \in \{0, 0.1, 0.2, 0.3, 0.4\}$  of the factor  $\xi$ . These values are in the range of demand uncertainties we observed in practice. For each of the resulting combinations of scenario and degree of stochasticity, we draw  $S = 1,000$  demand matrices  $\mathbf{d}^s$  with  $s \in \{1, \dots, S\}$  as realizations of  $[D_{ijt}]_{Z \times Z \times T}$  and use them to evaluate the ADP-H and ROL-H solution approaches, that is, to evaluate the price table that was optimized for the corresponding base demand matrix  $\mathbf{d}$ . Online Appendix G contains all results with confidence intervals.

Figure 7 illustratively depicts the results for  $\delta = 2/6$  and the three different zone numbers. On the vertical axis, the mean value of the relative profit increase with respect to the CUP benchmark (0% line) is depicted for ROL-1, ROL-8, ADP-1, and ADP-8. On the horizontal axis, the standard deviation  $\sigma$  is varied.

Overall, the proposed pricing approaches and our results are robust to the stochasticity of demand. However, all profit increases tend to decrease slightly with increasing stochasticity. The more sophisticated procedures are obviously more sensitive to stochasticity than CUP. However, these reductions in profit increase amount to at most two percentage points compared with zero stochasticity ( $\sigma = 0$ ), and the order of the different approaches regarding their performance does not change with increasing stochasticity. All proposed approaches still perform substantially better than the benchmark CUP, and as in Section 5.3.2, the anticipatory approach ADP-8 we propose is always the best.

As a technical remark, in the stochastic demand model, demand realization  $D_{ijt} < 0$  could potentially result, in particular, for high values of  $\sigma$  (see the corresponding discussion in Talluri and van Ryzin 2004, chapter 7.3.4). We correct for this by setting negative draws to zero. The small positive bias resulting from this truncation is not relevant to our study, because for each degree of stochasticity, we use the same 1,000 scenarios for all approaches we compare.

**Figure 7.** (Color online) Stochastic Evaluation of Solution Approaches in 9-, 16-, and 25-Zones Setting with Demand-Supply-Ratio  $\delta = 2/6$



Notes. (a)  $Z = 9$ . (b)  $Z = 16$ . (c)  $Z = 25$ .

### 5.3.6. Assessment of Pricing Approaches Covered in the Literature.

As stated in Section 1, the OBDPP, despite its relevance for practice, which we trace to the pricing approach's advantages compared with others, is a novel problem that has not been discussed in the literature yet. Thus, a *direct* comparison with pricing approaches covered in the literature is not feasible. Still, in this section, we assess pricing solutions *derived* from pricing approaches suggested in the literature to determine whether they could be applied to the problem at hand.

We explained in Section 2.3 that all the closest related studies differ from the OBDPP on two decisive points: The existing studies consider *trip-based* pricing instead of *origin-based* pricing, and they do not make the two central assumptions of *pure pricing* and *proportional demand fulfillment* (see Section 1). Therefore, we formulate two variants of the original OBDPP model (1)–(16):

- **TBDPP-RLX** mimics *trip-based* pricing (TBDPP) as the closest related work suggests (see Section 2.3). Similar to all of these studies, the model omits, or technically speaking, *relaxes* (RLX), the *pure pricing* and *proportional demand fulfillment* assumptions that are operative in the original OBDPP model. The TBDPP-RLX is formulated by (34)–(44) in Online Appendix H.1.

- **OBDPP-RLX** considers *origin-based* pricing as in the OBDPP but also *relaxes* the *pure pricing* and *proportional demand fulfillment* assumptions. By relaxing the OBDPP's two central assumptions, this model allows us to assess the two assumptions' realistic modeling in the OBDPP in isolation. The OBDPP-RLX is formulated by (45)–(55) in Online Appendix H.2.

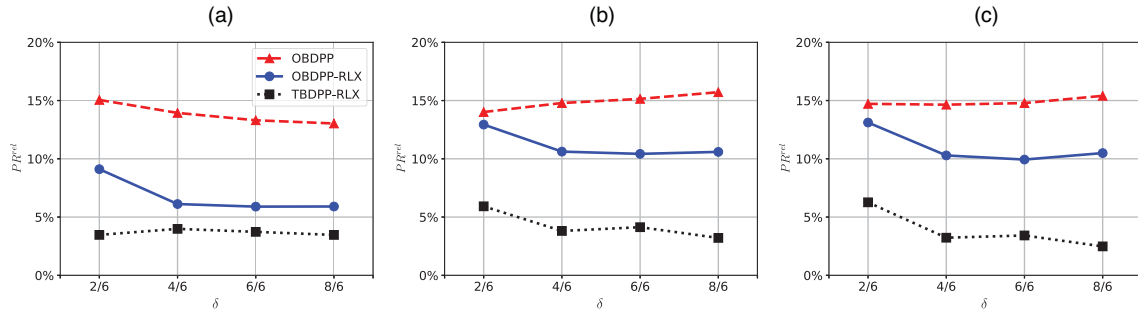
To assess the pricing solutions derived from the TBDPP-RLX and the OBDPP-RLX, we evaluate the resulting pricing solutions in the OBDPP and compare the resulting profits with the result we achieved by solving the OBDPP with our ADP decomposition approach (ADP-8). For the TBDPP-RLX, we determine origin-based prices from the trip-based pricing solution as follows:

In a first step, for every location-period combination, all corresponding trip-based prices are averaged. In the second step, the nearest price point from the given price set is determined. Regarding the solution methods for the OBDPP-RLX and the TBDPP-RLX, all periods of the respective problems are solved simultaneously (as for OPT and UB) with a computation time limit of 48 hours. Because of the reduced complexity of these two problems compared with the OBDPP, they can be solved close to optimally for all settings and scenarios: All solutions have a gap of less than 0.5% to the respective best known upper bound.

Figure 8 states the results for the three settings with 9, 16, and 25 zones, where each has four scenarios with different demand-supply ratios. Independent of the setting and scenario, the pricing determined by TBDPP-RLX performs worst of all pricing approaches. Also, the pricing determined by OBDPP-RLX is consistently worse than the one that OBDPP determined. In terms of profit  $PR^{rel}$  (percentage points with respect to (w.r.t.) CUP), pricing solutions delivered by OBDPP-RLX perform 0.1 to 7.2 percentage points worse than those of ADP-8, and the ones delivered by TBDPP-RLX perform 7.8 to 12.8 percentage points worse than those of ADP-8. This is because the OBDPP-RLX and especially the TBDPP-RLX suppose too high an influence on the resulting rentals than is possible in reality. Without the *pure pricing* and *proportional demand fulfillment* assumptions, the models can perform a kind of *availability control* (see Section 1). This means that rentals do not, as in reality, realize solely from dependence on the prevailing supply and demand but that the model can decide to reject certain rentals and to favor others that have specific destinations. For the TBDPP-RLX, this effect is even stronger, because the model can influence demand more flexibly with trip-based prices (location-location-period level), whereas in reality, prices are limited to being origin based (location-period level).

Overall, these results clearly justify two findings: First, pricing approaches such as those suggested in

**Figure 8.** (Color online) Comparison of Profit Obtained by Pricing Solutions with OBDPP, OBDPP-RLX, and TBDPP-RLX in Settings of 9, 16, and 25 Zones with Different Demand-Supply-Ratios  $\delta$



Notes. (a)  $Z = 9$ . (b)  $Z = 16$ . (c)  $Z = 25$ .

the literature (TBDPP-RLX) cannot be applied to determine prices for the OBDPP. Second, the exact modeling of the two central assumptions as they are prevalent in the reality of the OBDPP is indeed decisive in determining the best possible pricing solutions.

These results do not allow any statements regarding the effectiveness of origin-based pricing in comparison with *actual* trip-based pricing of an SMS. Clearly, if an SMS provider were able to put trip-based pricing into practice, this cannot perform worse than origin-based pricing, simply because of the additional flexibility. However, as explained in Section 1, practice, for very good reasons, exclusively applies origin-based pricing.

## 6. Case Study

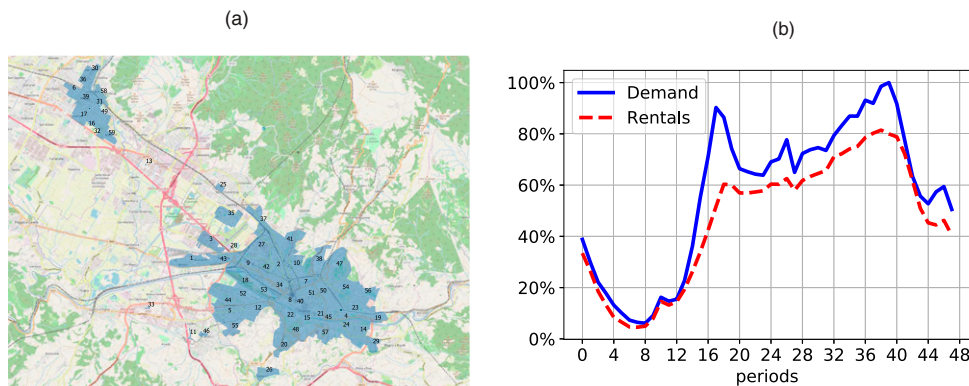
In this section, we consider a real-world scenario that reflects the origin-based differentiated pricing optimization of Share Now for a weekday in Florence, Italy. On the one hand, this case study allows us to conclude results and managerial insights in an instance of real-world size. On the other hand, compared with the rather stylized scenarios given in Section 5, all

parameters in this case study are based on real historic data that were collected over several months at Share Now. We introduce the scenario in Section 6.1 and discuss the results in Section 6.2.

### 6.1. Scenario and Parameters

Share Now's area of operation in Florence is divided into 59 zones, as shown in Figure 9(a). To respect the nondisclosure agreement, we only share values for demand and rentals that are normalized to the maximum period demand  $\max(d_t)$ , where  $d_t = \sum_{i,j \in Z} d_{ijt}$ . Figure 9(b) depicts the normalized base demand ( $d_t / \max(d_t) \forall t \in T$ ) and the resulting normalized rentals with the uniform pricing solution ( $\sum_{i,j \in Z} r_{ijt}^{(2)} / \max(d_t) \forall t \in T$ ) during the course of the day. The day is discretized into 48 periods of 30 minutes each. The demand curve shows the typical pattern with two peaks at the rush hour times, in the morning at  $t = 17$  (0830 hours) and in the evening at  $t = 39$  (2130 hours), with the lowest level during the night at  $t = 8$  (0400 hours). The rental curve follows the general course of the demand curve, with less pronounced peaks. During the night, the difference between demand and

**Figure 9.** (Color online) Share Now Scenario in Florence, Italy



Notes. (a) Operating area with 59 zones. (b) Normalized demand and rentals over the course of the day.

**Table 5.** Results from a Real-Life Scenario in Florence, Italy (59 Zones)

Solution approach	Change w.r.t. CUP			$P_{pm}^{prop}$			$RT_{pm}^{prop}$		
	$PR^{rel}$	$RV^{rel}$	$RT^{rel}$	Low	Base	High	Low	Base	High
ROL-1	3.9%	0.9%	-8.2%	11.1%	45.7%	43.2%	8.5%	33.5%	58.1%
ADP-1	7.0%	4.1%	-4.4%	8.8%	54.0%	37.1%	6.0%	43.2%	50.8%
ROL-4	6.8%	4.0%	-4.3%	8.4%	56.1%	35.5%	5.4%	45.5%	49.1%
ADP-4	9.2%	6.2%	-2.8%	13.7%	45.3%	41.0%	6.4%	41.1%	52.5%

rentals is smaller than during the day. This can be explained by the higher availability of vehicles during the night, implying that potential customers almost always find an available vehicle. During the day, in particular during peak times, the probability that demand results in a rental is lower because of the relatively high number of vehicles in use. The demand-supply-ratio in this scenario is approximately  $\delta = 0.7$ , which is in the range of scenarios with  $\delta < 1$  on which we focused in the computational experiments we described in Section 5.

Demand parameters are obtained from data Share Now recorded in April and May 2018. More precisely, the base demand matrix  $\mathbf{d}$  with entries  $d_{ijt}$  results from unconstraining the constrained demand, that is, the observed rentals. Unconstraining is a standard issue in revenue management (Talluri and van Ryzin 2004, chapter 9.4). We chose all other parameters as in the computational experiments (Section 5.1). The only difference concerns the VFA design and its parameter estimation process. We increased the number of pieces to  $K = 20$  to adapt to the larger fleet size. Finally, we compared our ADP decomposition approach's results in the ADP-4 configuration to the myopic benchmark ROL-1.

## 6.2. Results

Section 6.2.1 discusses the profit increase from ADP-4. Section 6.2.2 analyzes the resulting pricing decisions, rentals, and revenue.

**6.2.1. Profit.** Table 5 summarizes the  $PR^{rel}$  results for the Florence scenario. With our ADP decomposition

approach (ADP-4), the profit improvement  $PR^{rel}$  is 9.2%. Thus, the explicit and implicit consideration of network effects in ADP-4 realized an additional improvement of 5.3 percentage points compared with the myopic solution ROL-1 and an improvement of 2.4 percentage points over the ROL-4 benchmark. These results demonstrate the scalability of our solution approach to real-life scenarios and show a substantial improvement potential compared with the de facto standard of CUP through network effect consideration.

**6.2.2. Pricing Decisions, Rentals, Revenue.** We now analyze the effect of optimization on the pricing decisions, the rentals, and the revenue. Figure 10(a) depicts the  $PR_{pm,t}^{prop}$  results of ADP-4 during the course of the day and shows that the prices vary considerably. The largest proportion of highly priced rentals is set at demand peak times  $t = 17$  and  $t = 40$ . At non-peak times, the base price accounts for the largest proportion of rentals, with an exception in the very first period only. Table 5 shows the price proportions  $P_{pm}^{prop}$  over the whole day. We observe that, on average, ADP-4 leads to higher prices compared with the CUP benchmark, lower average prices compared with the myopic solution ROL-1, and comparable prices with ROL-4.

To gain more insight, we now illustratively consider four zones in more detail. Figure 11 depicts absolute demand, absolute available vehicles, and the prices of the ADP decomposition solution ADP-4 over all periods for the four zones with indexes 2, 7, 49, and 59. Zones 2 and 59 are characterized by relatively low

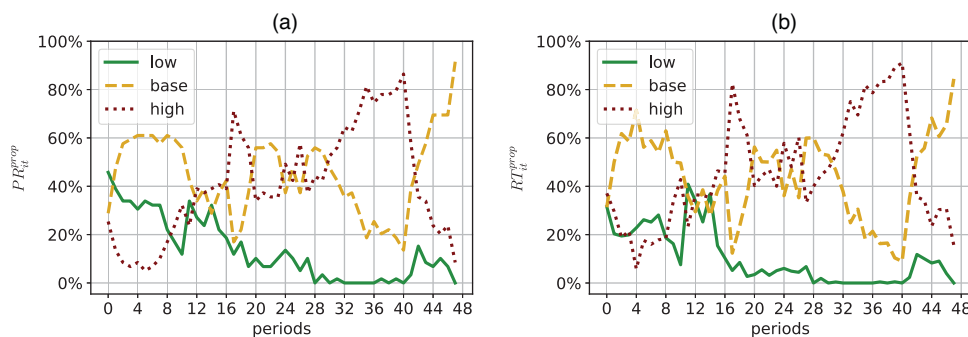
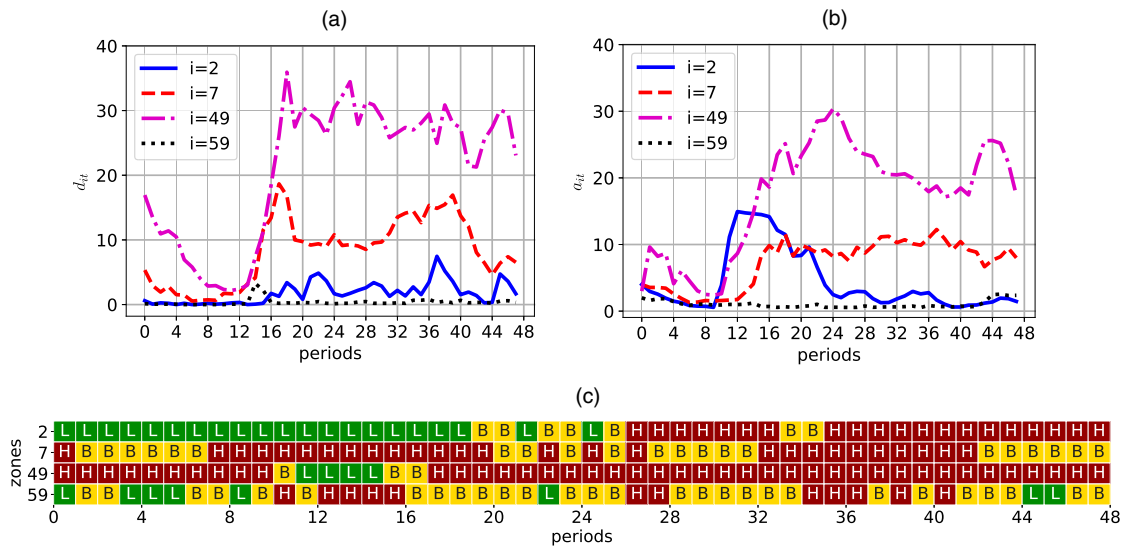
**Figure 10.** (Color online) Prices (a) and Rentals (b) over the Course of the Day (ADP-4)

Figure 11. (Color online) Base Demand (a), Available Vehicles (b), and Prices (c) in Four Selected Zones (ADP-4)



Notes. B, base price; H, high price; L, low price. (a) Base demand  $d_{it}$ . (b) Available vehicles  $a_{it}$ . (c) Prices  $p_{it}$ .

demand, zone 49 has the highest demand of the four, and zone 7's demand lies approximately halfway between the two extremes. During the first half of the day, especially during the morning peak time, zone 2 has relatively many vehicles available: more than the demand requires. This results in low prices at the beginning of the day and a declining vehicle count toward midday. During the evening peak, the levels of supply and demand are largely balanced, and high prices are set. Zone 7 shows the typical demand pattern, with two peaks that exceed the available vehicle count at these times. The resulting prices also show this shortage of vehicles at peak times, as high prices are set during these periods. Zone 49 has a higher demand than vehicle supply during most periods of the day and therefore often has high prices. The only exception is during the morning peak, when many vehicles arrive in that zone and lower prices are set to compensate for the oversupply. Zone 59 is characterized by relatively low demand and only a few available vehicles throughout the day, with high prices at peak times and low prices in the first periods. These observations show that the resulting pricing decisions differ considerably in their patterns. To some extent they can be explained by current supply and demand, but regarding the previously mentioned differences between the  $P_{pm}^{prop}$  of the myopic benchmark and the ADP decomposition approach, they are also the result of network effect considerations.

Table 5 shows that  $RT^{rel}$  decreases by 8.2% with the myopic solution and by 2.8% with the ADP decomposition approach solution, whereas  $RV^{rel}$  increases by 0.9% and 6.2%, respectively. Considering these figures in combination with the  $P_{pm}^{prop}$  discussed previously, the

additional  $PR^{rel}$  increase through network effect consideration of ADP-4 with respect to ROL-1 is a result of overall lower prices with more rentals and revenue. Figure 10(b) displays the  $RT_{pm}^{prop}$  of ADP-4. Their courses over the day resemble the courses of the respective  $PR_{pm}^{prop}$ . More precisely, during peak times, most of the rentals take place at a high price and in almost all other times most rentals are at the base price.

To summarize the results of the case study of Share Now in Florence, our solution approach generates considerably higher profits compared with the de facto standard of constant uniform prices and, more importantly, to the myopic benchmark. In fact, our solution even gets quite close to a theoretical upper bound. This increase is realized by a considerable price differentiation that allows for generating more revenue with fewer rentals in comparison with CUP at base price. High prices exploit the higher demand at peak times, and the larger proportion of low and base prices under network effect consideration allows for creating a more favorable fleet distribution and more rentals compared with the myopic solution.

## 7. Managerial Insights

The systematic computational experiments (abbreviated as *experiments*) of OBDPP scenarios given in Section 5 in combination with the analyses of the Share Now case study (abbreviated as *case*) given in Section 6 reveal important managerial insights for shared mobility providers, which we summarize in this section.

*Benefit of origin-based differentiated minute pricing:* The results demonstrate that origin-based differentiated minute pricing is more advantageous than constant uniform pricing that is still the de facto industry

standard. With our approximate dynamic programming decomposition solution approach, profits consistently increased throughout the considered instances, that is, in both experiments (10%–15%) and in the case (9%). For SMS providers, this is an insightful outcome, because origin-based differentiated minute prices are the first natural extension going beyond constant uniform prices. This is mainly because compared with other pricing mechanisms, origin-based differentiated pricing is relatively simple to implement, does not require upfront information about a trip's destination, and, very importantly, is easy to communicate to customers.

*Scalability requires sophisticated solution approaches:* The problem is computationally complex. More precisely, determining profit-maximizing pricing solutions is NP-hard. This is reflected by the fact that a straightforward solution using out-of-the-box commercial solvers is not possible. The supposedly obvious idea of directly solving the pricing problem in an integrated way, that is, simultaneously for all locations and in a reasonable time frame (e.g., a day), already fails for the smallest SMS that consists of only a few dozen locations. The standard next step is temporal decomposition, that is, considering multiple smaller problems with fewer periods instead of the entire day. This has a reasonable run time but in general lacks in solution quality. We show that more sophisticated approaches are necessary and possible, thereby striking a balance between the ideas of integrated and decomposed problem solving. In particular, our approximate dynamic programming decomposition approach provides a computationally tractable means for SMS providers applicable in instances of real-life size.

*Importance of network effect consideration:* The consideration of network effects is decisive for high-quality solutions. Our results demonstrate that SMSs are characterized by a complex interaction between supply and demand. Consequently, vehicle values differ considerably across locations and time. Furthermore, additional available vehicles at the same location and time have a decreasing marginal value because of limited demand. In contrast to straightforward pricing approaches like a myopic optimization, our approximate dynamic programming decomposition approach yields very good solutions that are close to an upper bound for the optimal solution. Key is its design for and ability to capture these network effects. This led to a profit increase over myopic pricing of up to 9.4 percentage points in the experiments and up to 5.3 percentage points in the case. These profit improvements depend on the instance. Especially for ratios of supply and demand prevalent in practice, there is a considerable improvement. Marginal vehicle values vary considerably in the range of 0 to 9.8 monetary units, which is equivalent to two to three rentals at base price where profit is 3.4 monetary

units. For SMS providers, the different marginal vehicle values provide a means of quantifying short- and long-term network effects, and they are also informative for other planning tasks, such as relocation.

*Profit increase because of price and quantity effect:* Profit maximization is not always equivalent to an increase in rentals. In the experiments, we indeed observed an increase of both profit and rentals for the best solutions we found. In the case, however, the profit increase was realized with less rentals and higher prices. For SMS providers, this is an important observation, because it also affects other service-oriented metrics like the availability of vehicles.

*High degree of price differentiation:* Finally, we observe that the best pricing solutions have a high degree of differentiation across time and space. In the case, for example, over all location-time combinations, we have an average of 15% low, 45% base, and 40% high prices. These proportions do not remain constant throughout the day. A deeper analysis of the price table revealed that some zones have high prices during the morning and evening rush hours, whereas others have lower prices at these times. We showed that these different pricing patterns result from the supply and demand level in these zones over time but are also a consequence of network effects. All these aspects indicate that the optimal price tables are complex. From a customer perspective, switching from constant uniform pricing to origin-based differentiated minute pricing means that prices now vary frequently. Therefore, it is important for SMS providers to accompany the introduction of origin-based minute price differentiation with a communications campaign that thoroughly explains the reasons for and benefits of the new approach, that is, to ensure customer satisfaction and loyalty.

## 8. Conclusion and Outlook

Motivated by our collaboration with Share Now, in this paper, we defined and analyzed the problem of origin-based differentiated pricing for SMSs. The paper has addressed the problem of determining spatially and temporally differentiated origin-based minute prices to maximize profit. Despite such price differentiation increasingly being adopted in practice, the research literature has not yet focused on these origin-based pricing mechanisms.

To model the SMS, we proposed a MILP based on a fluid formulation in which vehicle movements are described as flows through a spatio-temporal network. It naturally incorporates network effects, that is, the complex interactions between the moving vehicle supply and varying demand in an SMS. The problem turns out to be NP-hard; thus, heuristic solution

approaches are warranted. We therefore proposed an approach that simultaneously scales to real-life scenarios and approximately incorporates the network effects. We designed the approach in such a way that it combines the benefits of decomposition on the one hand and VFA from the realm of approximate dynamic programming on the other. The decomposition allows providers to quickly solve multiple smaller problems with limited time horizons instead of the original problem that simultaneously considers all periods. At the end of the considered horizon, a VFA allows for endogenously incorporating the profit-to-come in dependence of any resulting vehicle distribution.

Extensive computational experiments with a varying number of zones, demand patterns, and overall demand levels demonstrated the benefit of our approach. It considerably improves profit (up to 15%) compared with the de facto standard of constant uniform prices and compared with a myopic benchmark without consideration of network effects (up to 10 percentage points). In settings where the optimal solution can be determined, our approach finds a solution close to optimality. The resulting price tables show high similarity to the optimal price tables, in contrast to the price tables from the myopic pricing approach. We further demonstrated that the proposed VFA structure can reflect the decreasing marginal value of vehicles, which allows taking into account both short-term and long-term network effects.

In a real-life case study based on Share Now data, we demonstrated the scalability and performance of our solution approach. Profits increase 9% with respect to the de facto industry standard, although rentals decrease by 3%, leading to higher vehicle availability and 6% more revenue: two additional important operative indicators for SMS providers. Therefore, this illustrates that profit increases can result from price and quantity effect to the extent that profit increases can also realize with reduced rentals. A detailed analysis of prices showed considerable differentiation across the location-time combinations and that there are various price patterns in the different zones. SMS providers should bear this in mind when introducing origin-based differentiated minute pricing, as frequent price changes could affect the customer experience. Also, the consideration of network effects in our approach causes an overall price reduction compared with the myopic solution, resulting in more rentals and revenue. Considering both profit and pricing, we conclude that simple pricing rules cannot exploit the total potential for increased profit. We refer the reader to Section 7 for a generalized discussion of managerial insights that follow from jointly considering our computational experiments and the case.

To summarize, this work demonstrates the potential of origin-based differentiated minute pricing in SMSs and the importance of considering network effects. Our ADP decomposition approach provides a scalable means for integrating these effects successfully.

Based on the presented results and methodology, we believe there are several promising directions for future work. First, the fleet of car sharing providers typically consists of different vehicle types that could be represented in a formulation based on multicommodity network flow problems. Second, although our approach has already proved to be robust in a stochastic setting, developing approaches explicitly based on stochastic optimization models could be another useful way of extending our work and potentially further improving the promising results. Third, we believe that integrating VFAs in the vast field of other tactical and operational decision-making problems in SMSs is promising. This applies in particular to dynamic problems that require decision making in real time and reveals the problem of provider-based relocation, potentially in combination with pricing, as a relevant topic for future work.

### Acknowledgments

The authors thank Dr. Christian Mathissen, Head of Business Intelligence & Data Analytics at Share Now, and Dr. Alexander Baur, Team Lead Analytical Pricing & Revenue Management at Share Now, for support, valuable input, and fruitful discussions related to the authors' pricing project.

### References

- ACEA Frost & Sullivan (2016) Number of vehicles in global car sharing market from 2006 until 2025. *Statista*. Accessed September 1, 2020, <https://de.statista.com/statistik/daten/studie/388012/umfrage/anzahl-der-fahrzeuge-auf-dem-weltweiten-carsharing-markt/>.
- Agatz N, Campbell AM, Fleischmann M, Van Nunen J, Savelsbergh M (2013) Revenue management opportunities for Internet retailers. *J. Revenue Pricing Management* 12(2):128–138.
- Angelopoulos A, Gavalas D, Konstantopoulos C, Kyriadiis D, Pantziou G (2016) Incentivization schemes for vehicle allocation in one-way vehicle sharing systems. *Proc. IEEE Internat. Smart Cities Conf.* (IEEE Computer Society, Washington, DC), 1–7.
- Banerjee S, Freund D, Lykouris T (2021) Pricing and optimization in shared vehicle systems: An approximation framework. *Oper. Res.*, ePub ahead of print November 18, <https://doi.org/10.1287/opre.2021.2165>.
- Barth M, Todd M, Xue L (2004) User-based vehicle relocation techniques for multiple-station shared-use vehicle systems. Working paper, UC Riverside, Riverside, CA.
- Bertsekas DP (2019) *Reinforcement Learning and Optimal Control* (Athena Scientific, Belmont, MA).
- Brendel AB, Brauer B, Hildebrandt B (2016) Toward user-based relocation information systems in station-based one-way car sharing. *AMCIS Proc.* (Association for Information Systems, Atlanta), 1–10.
- Brendel AB, Brennecke JT, Zapadka P, Kolbe LM (2017) A decision support system for computation of carsharing pricing areas and its influence on vehicle distribution. *Proc. Internat. Conf. Inform. System* (Association for Information Systems, Atlanta), 1–21.



- Chemla D, Meunier F, Pradeau T, Wolfler Calvo R, Yahiaoui H (2013) Self-service bike sharing systems: Simulation, repositioning, pricing. Working paper, CERMICS, École des Ponts ParisTech, Champs-sur-Marne, France.
- DeMaio P (2009) Bike-sharing: History, impacts, models of provision, and future. *J. Public Transportation* 12(4):41–56.
- Di Febraro A, Sacco N, Saeednia M (2012) One-way carsharing. *Transportation Res. Rec.* 2319(1):113–120.
- Di Febraro A, Sacco N, Saeednia M (2019) One-way car-sharing profit maximization by means of user-based vehicle relocation. *IEEE Trans. Intelligent Transportation Systems* 20(2):628–641.
- Ferrero F, Perboli G, Vesco A, Caiati V, Gobbato L (2015a) Car-sharing services: Part A taxonomy and annotated review. Working paper, Istituto Superiore Mario Boella, Turin, Italy.
- Ferrero F, Perboli G, Vesco A, Musso S, Pacifici A (2015b) Car-sharing services: Part B business and service models. Working paper, Istituto Superiore Mario Boella, Turin, Italy.
- Fishman E, Washington S, Haworth N (2013) Bike share: A synthesis of the literature. *Transportation Rev.* 33(2):148–165.
- Garey MR, Johnson DS (1990) *Computers and Intractability: A Guide to the Theory of NP-Completeness* (W. H. Freeman & Co., New York).
- Giorgione G, Ciari F, Viti F (2019) Availability-based dynamic pricing on a round-trip carsharing service: an explorative analysis using agent-based simulation. *Proc. Comput. Sci.* 151(2018): 248–255.
- Grossmann IE (2012) Advances in mathematical programming models for enterprise-wide optimization. *Comput. Chemical Engrg.* 47: 2–18.
- Haider Z, Nikolaev A, Kang JE, Kwon C (2018) Inventory rebalancing through pricing in public bike sharing systems. *Eur. J. Oper. Res.* 270(1):103–117.
- Hardt C, Bogenberger K (2021) Dynamic pricing in free-floating car-sharing systems: A model predictive control approach. *Proc. Transportation Res. Board 100th Annual Meeting*.
- Huang K, Kun A, Rich J, Ma W (2020) Vehicle relocation in one-way station-based electric carsharing systems: A comparative study of operator-based and user-based methods. *Transportation Res. Part E: Logist. Transportation Rev.* 142:102081.
- Illgen S, Höck M (2019) Literature review of the vehicle relocation problem in one-way car sharing networks. *Transportation Res., Part B: Methodology* 120:193–204.
- Jorge D, Correia GHDA (2013) Carsharing systems demand estimation and defined operations: A literature review. *Eur. J. Transportation Infrastructure Res.* 13(3):201–220.
- Jorge D, Molnar G, Correia GHDA (2015) Trip pricing of one-way station-based carsharing networks with zone and time of day price variations. *Transportation Res., Part B: Methodology* 81:461–482.
- Kamatani T, Nakata Y, Arai S (2019) Dynamic pricing method to maximize utilization of one-way car sharing service. *Proc. IEEE Internat. Conf. Agent* (IEEE Computer Society, Washington, DC), 65–68.
- Kaspi M, Raviv T, Tzur M, Galili H (2016) Regulating vehicle sharing systems through parking reservation policies: Analysis and performance bounds. *Eur. J. Oper. Res.* 251(3):969–987.
- Laporte G, Meunier F, Wolfler Calvo R (2015) Shared mobility systems. *4OR* 13(4):341–360.
- Laporte G, Meunier F, Wolfler Calvo R (2018) Shared mobility systems: An updated survey. *Ann. Oper. Res.* 271(1):105–126.
- Lippoldt K, Niels T, Bogenberger K (2018) Effectiveness of different incentive models in free-floating carsharing systems: A case study in Milan. *Proc. IEEE Intelligent Transportation Systems Conf.* (IEEE Computer Society, Washington, DC), 1179–1185.
- Lippoldt K, Niels T, Bogenberger K (2019) Analyzing the potential of user-based relocations on a free-floating carsharing system in Cologne. *Transportation Res. Procedia* 37:147–154.
- Lu R, Correia GHDA, Zhao X, Liang X, Lv Y (2021) Performance of one-way carsharing systems under combined strategy of pricing and relocations. *Transportation B: Transportation Dynamics* 9(1):134–152.
- Marecek J, Shorten R, Yu JY (2016) Pricing vehicle sharing with proximity information. *Proc. 3rd MEC Internat. Conf. Big Data and Smart City* (IEEE Computer Society, Washington, DC), 1–7.
- Müller C, Gönsch J, Soppert M, Steinhardt C (2021) Customer-centric dynamic pricing for free-floating shared mobility systems. Working paper, University of Duisburg-Essen, Duisburg, Germany.
- Neijmeijer N, Schulte F, Tierney K, Polinder H, Negenborn RR (2020) Dynamic pricing for user-based rebalancing in free-floating vehicle sharing: A real-world case. Lalla-Ruiz E, Mes M, Voß S, eds. *Proc. Internat. Conf. Comput. Logist., Lecture Notes in Computer Science* (Springer International Publishing, Basel, Switzerland), 443–456.
- Pfrommer J, Warrington J, Schildbach G, Morari M (2014) Dynamic vehicle redistribution and online price incentives in shared mobility systems. *IEEE Transportation Intelligent Transportation Systems* 15(4):1567–1578.
- Powell WB (2009) What you should know about approximate dynamic programming. *Naval Res. Logist.* 56(3):239–249.
- Powell WB (2011) *Approximate Dynamic Programming*. Wiley Series in Probability and Statistics (Wiley, Hoboken, NJ).
- Powell WB (2016) Perspectives of approximate dynamic programming. *Ann. Oper. Res.* 241(1-2):319–356.
- Reiss S, Bogenberger K (2016) Optimal bike fleet management by smart relocation methods: Combining an operator-based with a user-based relocation strategy. *Proc. IEEE Intelligent Transportation Systems Conf.* (IEEE Computer Society, Washington, DC), 2613–2618.
- Ren S, Luo F, Lin L, Hsu SC, Li XI (2019) A novel dynamic pricing scheme for a large-scale electric vehicle sharing network considering vehicle relocation and vehicle-grid-integration. *Internat. J. Production Econom.* 218:339–351.
- Ricci M (2015) Bike sharing: A review of evidence on impacts and processes of implementation and operation. *Res. Transportation Bus. Management* 15:28–38.
- Roland Berger (2014) Shared mobility—How new businesses are rewriting the rules of the private transportation game. *Think Act* (Roland Berger Strategy Consultants GmbH, Munich, Germany).
- Share Now (2021) Overview countries and cities. *Share Now*. Accessed February 25, 2021, <https://www.share-now.com/de/en/country-list/>.
- Singla A, Santoni M, Bartok G, Mukerji P, Meenen M, Krause A (2015) Incentivizing users for balancing bike sharing systems. *Proc. 29th AAAI Conf. Artificial Intelligence Pattern*, 723–729.
- Soppert M, Steinhardt C, Müller C, Gönsch J (2022) Matching functions for free-floating shared mobility system optimization to capture maximum walking distances. Working paper, University of the Bundeswehr Munich, Neubiberg, Germany.
- Talluri KT, van Ryzin GJ (2004) *The Theory and Practice of Revenue Management* (Springer, Boston).
- Wagner S, Willing C, Brandt T, Neumann D (2015) Data analytics for location-based services: Enabling user-based relocation of car-sharing vehicles. *Proc. Internat. Conf. Inform. Systems*, vol. 3 (Association for Information Systems, Atlanta), 279–287.
- Wang L, Ma W (2019) Pricing approach to balance demands for one-way car-sharing systems. *Proc. IEEE Intelligent Transportation Systems Conf.* (IEEE Computer Society, Washington, DC), 1697–1702.
- Waserhole A, Jost V (2012) Vehicle sharing system pricing regulation: A fluid approximation. Working paper, ENSTA ParisTech, Palaiseau, France.

- Waserhole A, Jost V (2016) Pricing in vehicle sharing systems: Optimization in queuing networks with product forms. *EURO J. Transportation Logist.* 5(3):293–320.
- Waserhole A, Jost V, Brauner N (2012) Vehicle sharing system optimization: Scenario-based approach. Working paper, ENSTA ParisTech, Palaiseau, France.
- Winston WL, Goldberg JB (2004) *Operations Research: Applications and Algorithms*, vol. 4 (Thomson/Brooks/Cole, Belmont, CA).
- Xu M, Meng Q, Liu Z (2018) Electric vehicle fleet size and trip pricing for one-way carsharing services considering vehicle relocation and personnel assignment. *Transportation Res., Part B: Methodology* 111:60–82.